Funded by the European Union

Horizon Europe

EUROPEAN COMMISSION

European Climate, Infrastructure and Environment Executive Agency (CINEA)

Grant agreement no. 101056765

ev4eu

Electric Vehicles Management for carbon neutrality in Europe

Deliverable D1.8
Characterization of Batteries degradation considering the participation in V2X services

Document Details

Due date	30-04-2024
Actual delivery date	24-04-2024
Lead Contractor	Smart Energy Lab (SEL)
Version	1.0
Prepared by	Catarina Nogueira (SEL), Diogo Brito (SEL), Hugo Morais (INESC-ID)
Reviewed by	João Mateus (EDP NEW), Antonios Koutounidis (HEDNO)
Dissemination Level	Public

Project Contractual Details

Project Title	Electric Vehicles Management for carbon neutrality in Europe
Project Acronym	EV4EU
Grant Agreement No.	101056765
Project Start Date	01-06-2022
Project End Date	30-11-2025
Duration	42 months

Document History

Version	Date	Contributor(s)	Description
0.1	09-01-2024	SEL	Table of contents
0.2	15-04-2024	SEL, INESC-ID	Version completed for revision
0.3	24-04-2024	EDP NEW, HEDNO	Internal review
1.0	24-04-2024	SEL	Final version

Disclaimer

This document has been produced in the context of the EV4EU project. Views and opinions expressed in this document are however those of the authors only and do not necessarily reflect those of the European Union or the European Climate, Infrastructure and Environment Executive Agency (CINEA). Neither the European Union nor the grating authority can be held responsible for them.

Acknowledgment

This document is a deliverable of EV4EU project. EV4EU has received funding from the European Union´s Horizon Europe programme under grant agreement no. 101056765.

Funded by
the European Union

Executive Summary

The Deliverable D1.8 – *Characterization of Batteries degradation considering the participation in V2X services* deliverable presents an evaluation of electric vehicles (EV) battery degradation when different scenarios of vehicle-to-everything (V2X) are applied. This document presents a characterization of the new business models defined in Deliverable D1.4, that were the base for the V2X use cases repository with seven Business Use Cases (BUCs) defined in Deliverable D1.5. These use cases are the participation in frequency regulation services, V2X/Renewable Energy Sources (RES) coordination, and the participation in electricity markets through a virtual power plant, in dynamic contracts, and implicit and explicit demand response.

This study includes an overview of the main findings in the literature review performed on the battery degradation mechanisms, that are divided into calendar and cycle aging. The main variables that affect the battery's life, such as temperature, state-of-charge, charge and discharge rate, charge voltage, depth-of-discharge, and cycle frequency, are also presented.

Based on the use cases' demand and how the life of a battery is affected by how it's used, to simulate how in each scenario the battery would lose capacity and/or power, it was necessary to find a mathematical model that could be included in a simulation tool. Through an exhaustive review of literature to identify the most suitable model, it was determined that semi-empirical battery models stand out as the optimal tools for predictive analysis. This preference arises from the cost-prohibitive nature of empirical full life cycle testing. However, it is crucial to acknowledge that these semi-empirical models are inherently constrained by their source data. This means limitations in test conditions and the specific characteristics of the cells studied, including constraints in the chemistry, which can impact the accuracy of the final outcomes. Despite these, three models are presented in this document that have different characteristics, where the Wang model was the one chosen. To simulate the several scenarios, a Python library called Python Battery Mathematical Modelling (PyBaMM) was used, and the degradation model was included.

The main achievement of the present study is that it was possible to simulate using an existing model from the literature and real data from service characterization. This allowed us to understand that frequency regulation is the service that demands the most from a battery. This is evident in the need for rapid response to commands, which may not always be feasible. Additionally, it was observed that a higher frequency of deviations and longer durations contribute to increased cycle aging, thus leading to battery degradation. To mitigate the need of wind curtailment, it is important to coordinate the EVs charging with the periods when wind curtailment can occur. The other four use cases have similar needs in terms of batteries behaviour (charge and discharge profiles), which would mean a few cycles of charge and discharge in a day in the most demanding scenario.

Table of Contents

List of Figures

List of Tables

Acronyms

aFRR	Automatic Frequency Restoration Reserve
BM	Business Model
BRP	Balancing Responsible Party
BUC	Business Use Case
C&I	Commercial and Industrial
CHP	Combined Heat and Power
CPP	Critical Peak Pricing
CSP	Congestion Service Provider
DADRP	Day-Ahead Demand Response Program
DC	Direct Current
DER	Distributed Energy Resource
DoD	Depth-of-Discharge
DR	Demand Response
DSASP	Demand-Side Ancillary Services Program
DSO	Distribution System Operator
EAN	Electricity Allocation Number
EDA	Eletricidade dos Açores
EDRP	Emergency Demand Response Program
EIS	Electrochemical Impedance Spectroscopy
ENTSO-E	European Network of Transmission System Operators for Electricity
EV	Electric Vehicle
EV4EU	Electric Vehicles Management for Carbon Neutrality in Europe
FCR	Frequency Containment Reserve
FCR-D	Frequency Containment Reserve for Disturbances
FCR-N	Frequency Containment Reserve for Normal Operation
FFR	Fast Frequency Reserve
FR	Frequency Regulation
FSP	Flexibility Service Provider
GOPACS	Grid Operators Platform for Congestion Solutions
HPPC	Hybrid Pulse Power Characterization
IB	Incentive-based
IBDR	Incentive-Based Demand Response
ICAP-SCR	Installed Capacity – Special Case Resource
kWh	kilowatt-hour
LFP	Lithium Iron Phosphate
LiB	Lithium-Ion Battery
LMO-NMC	Lithium Iron Phosphate
mFRR	Manual Frequency Restoration Reserve

MOCIBUS	Modelling of Batteries Including the Coupling Between Calendar and Usage Aging
NCA	Lithium Nickel Cobalt Aluminium Oxides
NODES	New Energy Market Design
NREL	National Renewable Energy Laboratory
NYISO	New York Independent System Operator
PB	Price-Based
PBDR	Price-Based Demand Response
PyBaMM	Python Battery Mathematical Modelling
RES	Renewable Energy Source
RTP	Real-Time Pricing
SCE	Southern California Edison
SEI	Solid Electrolyte Interphase
SoC	State-of-Charge
ToU	Time-of-Use
TSO	Transmission System Operator
UC	Use Case
V2B	Vehicle-to-Building
V2G	Vehicle-to-grid
V2H	Vehicle-to-House
V2X	Vehicle-to-Everything
VPP	Virtual Power Plant

Nomenclature

A	Pre-exponential factor
$Ah_{throughput}$	Throughput capacity
B_1	Pre-exponential fitting factor
B_2	Exponential fitting factor
C_{rate}	Average C-rate
E_a	Activation energy
$Q_{calendar,\%}$	Calendar aging in a lithium-ion battery
$Q_{cycle,\%}$	Cycle aging in a lithium-ion battery
$Q_{loss,\%}$	Overall loss in a lithium-ion battery
R	Universal gas constant
$SoH_{model,\%}$	State-of-Health by the model
t	Time
T	Battery temperature
V_{OC}	Open-circuit voltage
q_T	Rate of Arrhenius dependence on temperature
q_{VOC}	Rate of Tafel dependence on open-circuit voltage
q_{DoD}	Rate of Whöler dependence on changes in depth-of-discharge

1 Introduction

1.1 Scope and Objectives

This document presents the study of battery degradation, considering the participation of electric vehicles (EVs) in several grid services. Based on an extensive literature review, this document assesses the impact these services would have on the battery life of an EV, used to deliver them.

The objectives of this work can be folded into four parts. First, it provides a characterization of each of the services, in frequency regulation (FR) with the Danish case, in wind curtailment with the Portuguese case, and then several European examples of the flexibility services, whether the local markets, electricity markets, dynamic contracts, and implicit and explicit demand response. These services have been selected based on the use cases identified in the project EV4EU. The characterization of the services allowed us to obtain real data of the first two services that helped to better understand its demands. Second, it gives an analysis of the main battery degradation mechanisms found in several scientific articles and previous studies, allowing an understanding of what happens in a battery depending on the surrounding conditions, and how it's used. Third, to simulate the battery degradation in each scenario it is necessary to find an adequate mathematical, semi-empirical model that combines the main degradation mechanisms and variables. The fourth and main goal is to perform several simulations considering the demands of each use case, to then find how it would affect the battery life in a real context.

To achieve the main objectives of this work, we carried out an extensive search of the existing literature regarding information about each of the services, battery degradation, main mechanisms and variables, and existing models. This information was obtained from documents published in several scientific journals, previous conferences, and the websites of power systems stakeholders (such as transmission system operators). When the information was not available, some assumptions have been taken concerning the battery degradation model, and the services that are intended to be studied, allowing the simulation of each of them.

1.2 Structure

This document is structured in the following way: Chapter 2 presents the different V2X scenarios, starting by describing each one, with the presentation of existing examples, and then presenting their main characteristics. In Chapter 3, a detailed explanation of how a lithium-ion battery (LiB) degrades, with focus on the two modes of degradation and how the functioning of a battery affects their characteristics. To understand how each scenario would affect the battery's life, in Chapter 4 a battery degradation model is presented. Chapter 5 then presents the performed simulations using the model previously presented for each vehicle-to-everything (V2X) scenario.

1.3 Relationship with other deliverables

Work Package 1 aims to define the road of e-mobility scenarios in a V2X context, with deliverables D1.4 [1], that defined the new business models (BM) for the project, and D1.5 [2] that developed a V2X use-cases repository with seven business use cases (BUCs) [3] based on those business models, which will then be tested in the project demonstrators sites in Denmark, Greece, Slovenia, and Portugal. The present deliverable takes the defined UCs that serve as an input to understand the battery degradation when those different scenarios of V2X are applied. For the service of wind curtailment, the work performed in deliverable D2.1 [4] was used to have the data necessary to then characterize it.

2 Grid Services

Grid services that can be provided by V2X can be generalized into energy-based products and power-based products. Bulk energy transfer products such as performing vehicle-to-grid (V2G) energy arbitrage (charging/buying electricity during times of low energy prices and discharging/selling during periods of high energy prices), providing V2G spinning reserves (bulk energy discharge or dynamically altering charge rate in response to grid requirements), acting as a demand response (DR) resource. Furthermore, V2X technologies can serve as emergency backup power through vehicle-to-home (V2H) and vehicle-to-building (V2B) solutions. All result in similar load profiles in that a large energy throughput is required which translated to long periods of charging or discharging of a vehicle battery. Frequency of use, daily timing, and utilization rate for each service will, however, differ. Power products (most notably V2G frequency regulation) where fast response time is crucial will result in significantly less energy exchange as the inherent energy service is charge/discharge flexibility [5].

In this deliverable the focus will be on the V2X BUCs defined in D1.5 [2], which are:

i. System Level V2X/RES Coordination.
ii. Participation of V2X in Frequency Regulation services.
iii. Participation of V2X in Electricity Markets through a Virtual Power Plant.
iv. Participation of V2X in Local Flexibility Markets.
v. Participation of V2X managers in Dynamic Contracts to support Distribution System Operator (DSO) operation.
vi. Participation of V2X in Explicit Demand Response to Congestion Management services.
vii. Participation of V2X in Implicit Demand Response to voltage control and V2X/RES coordination in distribution systems.

In the first BUC, System Level V2X/ Renewable Energy Source (RES) Coordination, the focus is on utilising V2X during Wind Curtailment.

To better comprehend the demands placed on a lithium-ion battery within each of the mentioned V2X services in this project, this chapter provides a characterization of these use cases with real data and examples when applied.

Section 2.1 presents what the concept of wind curtailment is, Section 2.2 presents the frequency regulation, and Section 2.3 presents the flexibility services, which are electricity markets, local markets, dynamic contracts, implicit demand response and explicit demand response.

2.1 Wind Curtailment

Wind curtailment refers to the situation where the output of wind plants is reduced to a level below its available generation capacity. This happens when the generation electricity mix is higher than the power consumption, where the generation electricity mix includes generation sources that cannot be reduced or turned off due to technological constraints without compromising the safety and stability of the entire system. In the case of the Azores, that is an isolated system, at least one thermal power group should be working for security purposes. When compared to wind systems, for which the output usually increases at night that is an off-peak period in terms of consumption. This means that there is a high possibility of oversupply. In this case, the transmission system operator (TSO) is forced to order curtailment to ensure the stable operation of the power system [6].

2.1.1 Portuguese Case (Azores)

From the four demonstrator countries in EV4EU project, it was decided to characterize the wind curtailment use case in Portugal, specifically in the São Miguel Island, where from Eletricidade dos Açores (EDA) and D2.1 [4] power data was obtained from a 9 MW wind farm, located in Graminhais. The collected sample extends from January 1st, 2022, to December 31st, 2022, at intervals of 10 minutes.

Figure 2.1 illustrates the average curtailed power at the Graminhais wind farm, per month and per time of day, focusing on the night period.

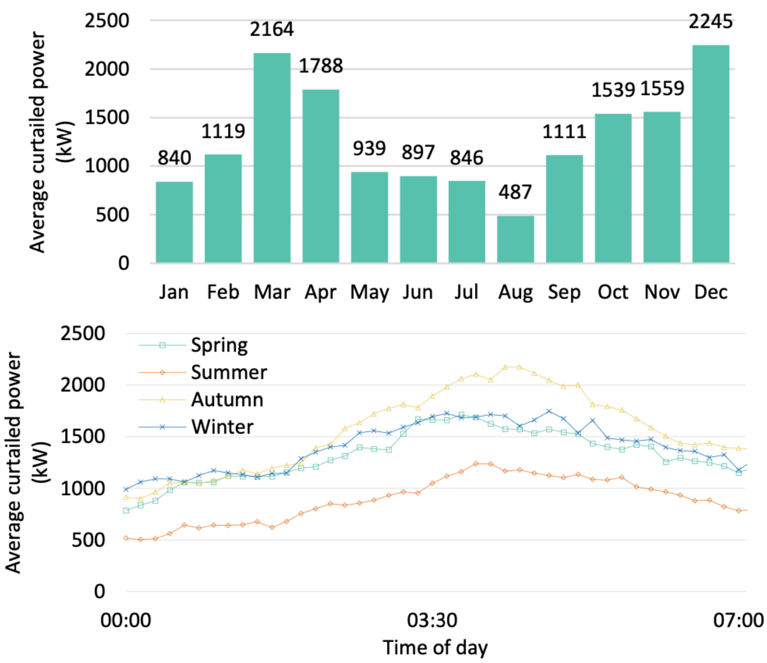

Figure 2.1: Average curtailed power at the Graminhais wind farm per month (top) and per time of day (bottom) [4].

As previously mentioned, curtailment in a wind farm typically happens during the night, which coincides with off-peak consumption times. Concurrently, home EV charging predominantly occurs during this period. By coordinating these two events, it's possible to mitigate or even avoid wind curtailment.

2.2 Frequency Regulation

Frequency stability is the ability of an electric system to regulate its frequency within the permitted/nominal operating range. Whereas frequency instability is often the result of an imbalance between the grid total generation and load. Frequency regulation ensures the balance of electricity supply and demand at all times, particularly over time frames from seconds to minutes. When supply exceeds demand, the electric grid frequency increases and vice versa [7].

In the synchronous areas that the ENTSO-E[1] (European Network of Transmission System Operators for Electricity) members are part of, the frequency regulation is divided into four different main products, called frequency containment reserve (FCR), or primary control reserve, automatic frequency restoration reserve (aFRR), or secondary control reserve, manual frequency restoration reserve (mFRR), or tertiary control reserve, and replacement reserve (RR) [8].

In the event of frequency deviations, the primary frequency regulation must ensure that the balance between generation and demand is restored, stabilising the frequency at close to, but deviating from 50 Hz. It's automatic and provided by generation or demand units which, by means of control equipment, respond to grid frequency deviations.

The secondary frequency regulation is a centralised automatically activated reserve. It activates based on an activation request signal sent by the TSO. The activation request is calculated based on the frequency deviation.

The tertiary control reserve intervenes when there are longer lasting deviations in the power grid that cannot be resolved solely by the other upstream balancing serves (FCR or aFRR).

Figure 2.2 presents a resume of the division of frequency regulation reserves with an example of frequency and power curves.

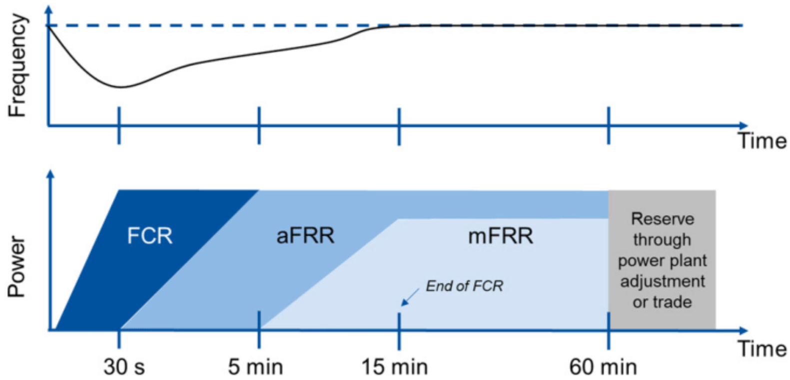

Figure 2.2: Division of frequency regulation with exemplary frequency curve (top) and power type responsibilities (bottom) based on [8].

2.2.1 Danish Case

Out of the four countries with demonstrators in this project, it was decided to make a characterization of the Denmark frequency regulation, due to being divided into two parts, DK1 and DK2. DK1 is the western Denmark part of the European power system (Continental synchronous area), and DK2 is the eastern Denmark part of the Scandinavian countries (Nordic synchronous area). The two areas are electrically connected through the direct current (DC) Great Belt Power Line, controlled by the Danish TSO, Energinet[2] [9]. However, considering that this link is made in DC, the areas can be decupled in term of frequency synchronization.

Figure 2.3 presents a map of the DK1 and DK2, and the frequency products that each part has.

[1] https://www.entsoe.eu
[2] https://en.energinet.dk/electricity/

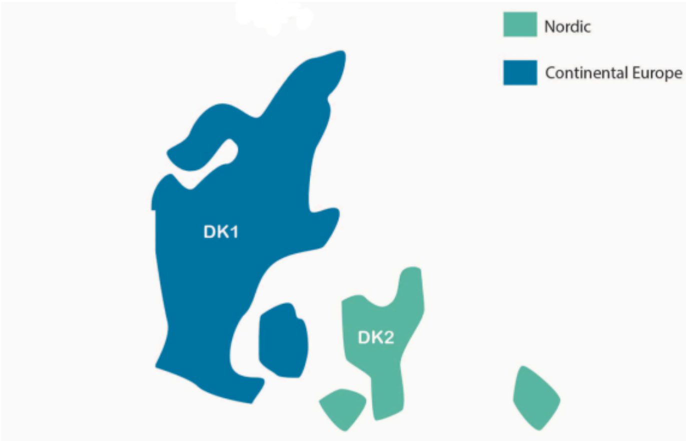

Process	Fast Frequency Reserve (FFR)		Frequency Containment Reserve (FCR)		Frequency Restoration Reserve (FRR)	
Automatic Product	NA	FFR	FCR	FCR-N FCR-D	aFRR	aFRR
Manual Product	NA	NA	NA	NA	mFRR	mFRR

Figure 2.3: Western Denmark (DK1) and Eastern Denmark (DK2) map [10].

In Denmark, frequency regulation is a service which is paid per availability. This means that the price is based on the power capacity that is available for an hour, in MWh, and not on the actual energy that is provided [9].

In DK1, the primary frequency regulation is conducted in the frequency range of ±200 mHz, with an operational dead band of ±20 mHz, relative to the reference frequency. The regulation service must be delivered linearly, with the maximum delivery time of 15 seconds for the first 50% capacity, and 30 seconds for the rest. In addition, each of up and down regulation services have a different set price, and the service must be able to stand for 15 minutes, and a cool down period of also 15 minutes [11].

On the other hand, in DK2, the primary frequency regulation is performed to stabilize the grid frequency close to the reference frequency. It also reduces the number of jumps/dips of frequency. This service will be automatically activated in any frequency deviation of ±100 mHz relative to the reference value. It is conducted as a fast-reacting proportional control and performed symmetrically. Moreover, there is no dead-band in frequency containment reserve for normal operation (FCR-N) and the maximum delivery time is 150 seconds, which can be performed continuously. Both primary frequency regulations in DK1 and DK2 are conducted based on a daily auction [11].

When it comes to secondary frequency regulation, both in DK1 and DK2, the aFRR reserves are used to indirectly restore the frequency to the normal band (50±0.1 Hz) following the stabilisation of the frequency by means of power frequency control. In the DK1, it must be possible to supply the aFRR reserve that was requested within 15 minutes, whereas in DK2 it should be within 5 minutes [12].

For DK2, there are two products of FCR, frequency containment reserve for normal operation (FCR-N) and frequency containment reserve for disturbances (FCR-D). Both are active power reserves that are automatically controlled based on the frequency deviation. Their purpose is to contain the frequency during normal operation and disturbances, respectively. FCR-N aims to keep the frequency within the standard frequency range of 49.9 Hz to 50.1 Hz. FCR-D aims to limit the frequency deviation to 49.5 Hz or 50.5 Hz when the frequency goes outside the standard range [12].

FCR-N is a symmetrical product that must be capable of both up- and down regulation. Upregulation means increasing power production or decreasing consumption. Downregulation means decreasing power production or increasing consumption. FCR-D is divided into separate up- and down regulation products [12].

Concerning the fast frequency reserve (FFR) service in DK2, in the event of major system disturbances in low inertia situations is used to regulate the frequency in case of substantial frequency drops resulting from the outage of major generation units or lines. It's necessary in situations with low inertia as frequency-controlled disturbance reserves in the Nordic synchronous area cannot by itself maintain the frequency above the specific threshold values. This reserve is activated automatically at frequency dips below 49.7/49.6/49.5 Hz and remains active until FCR-D has been fully activated [12].

When it comes to the manual reserve, or tertiary reserve, both in DK1 and DK2, it is a manual upward and downward regulation reserve, which is activated by the Danish TSO. It is activated through a manual order that requests for upward or downward regulation from the suppliers. This reserve relieves the aFRR and the FCR-N reserves in the event of minor imbalances and ensures balance in the event of outages or restrictions affecting generation units and interconnections [12].

Figure 2.4 presents a summary of frequency regulation in Denmark.

Frequency Regulation in Denmark (DK1 and DK2)					
FR Service	aFRR	FCR-N/FCR-D	FCR	mFRR	FFR
Service Duration	5-15min	150s/5-30s	15-30s	15min	1s

Figure 2.4: Summary of Frequency Regulation in Denmark, adapted from [13].

In order to characterise this service with real profile data, Netztransparenz.de[3], the information platform for Germany's TSOs, was used to obtain frequency data for the Continental synchronous area, of which DK1 is a part of. For the Nordic synchronous area, which includes DK2, the Open Data platform of Finland's TSO, Fingrid[4], was used to obtain its frequency data. One year of data was extracted in both cases, from October 2022 to October 2023.

Then, the frequency profiles for October 2022 and October 2023 for West Denmark were obtained, as presented in Figure 2.5 and Figure 2.6.

[3] https://www.netztransparenz.de/de-de/Regelenergie/Daten-Regelreserve/Sekündliche-Daten
[4] https://data.fingrid.fi/en/datasets/339

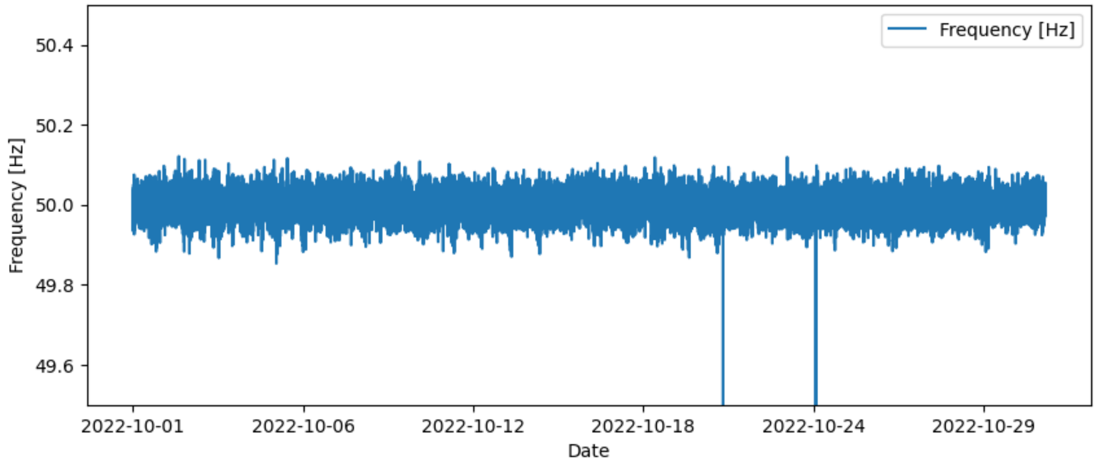

Figure 2.5: West Denmark's (DK1) frequency profile in October 2022.

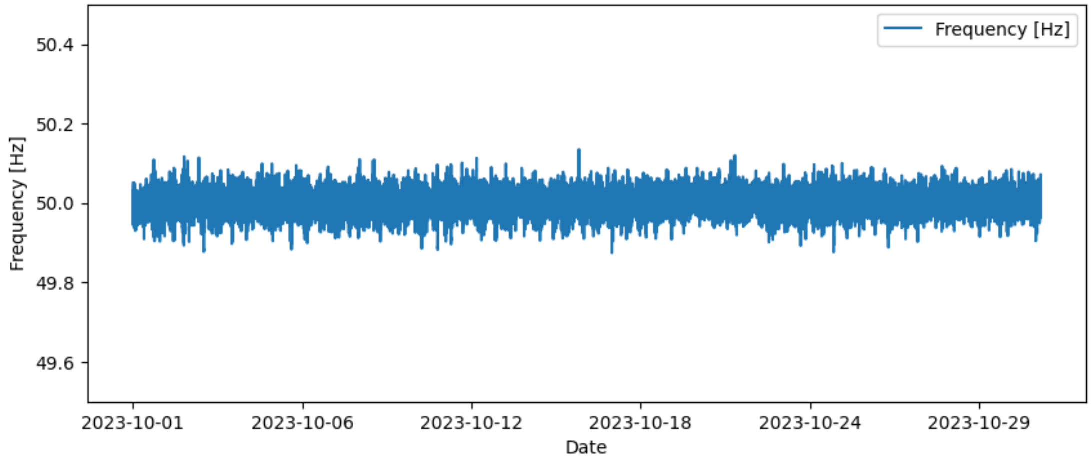

Figure 2.6: West Denmark's (DK1) frequency profile in October 2023.

In Figure 2.5 it can be observed that there are two events where the frequency deviated from the average value. These values were retrieved from the Continental synchronous area, and are therefore not a mistake in the graph, and were indeed moments where the frequency deviated more than the usual in that month from 50 Hz.

Table 2.1 shows a characterization of the frequency deviations outside the normal range of frequency (50±0.1 Hz), with the number of these deviations and the maximum time that was found in each month of a deviation during the studied year of data, in West Denmark.

Table 2.1: Characterization of frequency deviations in West Denmark (DK1) per month.

Month-Year	Number of frequency deviations outside 50±0.1 Hz	Maximum time duration of the deviations [s]
Oct-22	460	18
Nov-22	436	24
Dec-22	292	24
Jan-23	350	18
Feb-23	356	16
Mar-23	3878	334
Apr-23	3546	254
May-23	746	20
Jun-23	1058	74
Jul-23	696	48
Aug-23	1106	104
Sep-23	760	58
Oct-23	722	84

The frequency deviations accounted in Table 2.1 correspond to an average of 0.04% of deviations in a month, with an average duration of 83 seconds in the Continental synchronous area.

For East Denmark, the frequency profiles of the same months were obtained, and are presented in Figure 2.7 and Figure 2.8.

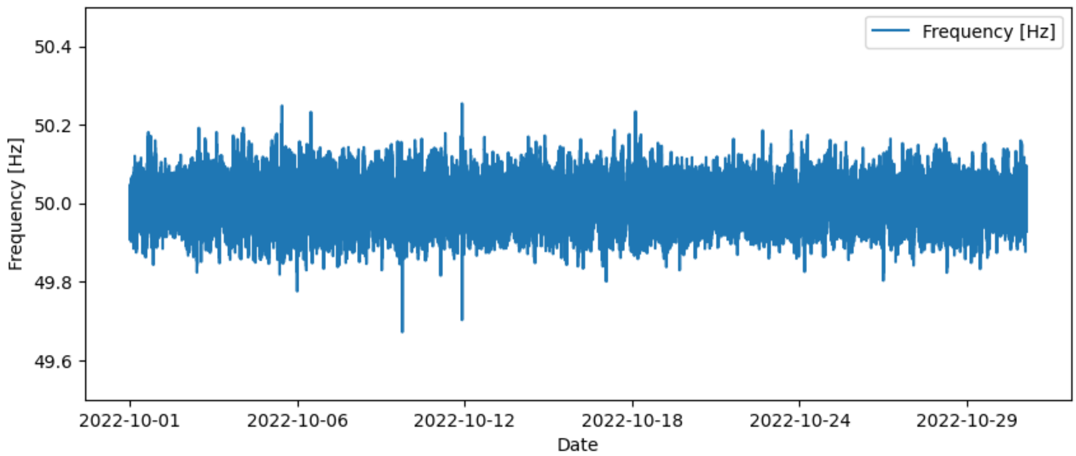

Figure 2.7: East Denmark's (DK2) frequency profile in October 2022.

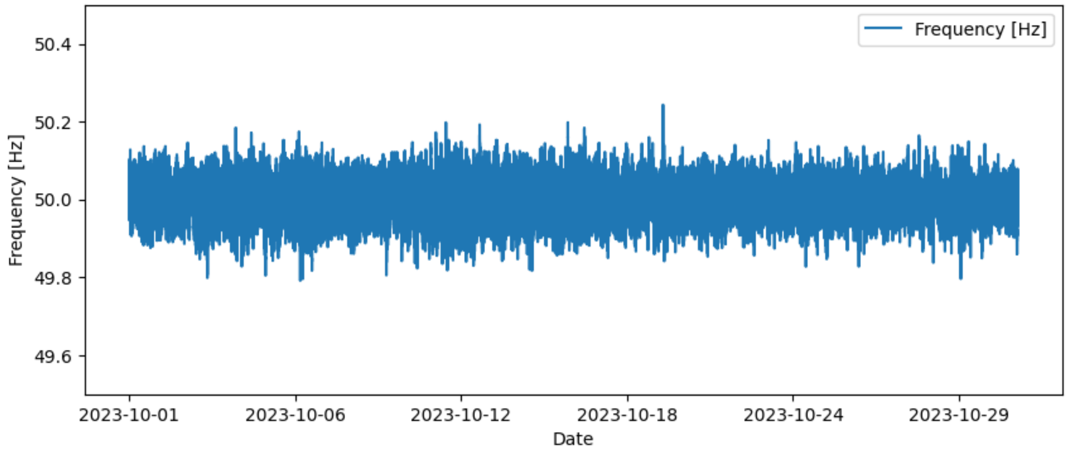

Figure 2.8: East Denmark's (DK2) frequency profile in October 2023.

Table 2.2 shows a characterization of the frequency deviations outside the normal range of frequency (50±0.1 Hz) during the studied year of data for East Denmark.

Table 2.2: Characterization of frequency deviations in East Denmark (DK2) per month.

Month-Year	Number of frequency deviations outside 50±0.1 Hz	Maximum time duration of the deviations [s]
Oct-22	56818	572
Nov-22	33709	535
Dec-22	39202	922
Jan-23	49819	628
Feb-23	39955	834
Mar-23	50875	504
Apr-23	61161	655
May-23	74967	442
Jun-23	53673	676
Jul-23	30933	731
Aug-23	46361	419
Sep-23	61488	670
Oct-23	42267	343

Where the frequency deviations accounted in Table 2.2 correspond to an average of 1.87% of deviations in a month, with an average duration of 610 seconds in the Nordic synchronous area.

2.3 Flexibility Services

Flexibility is the ability of a power system to maintain or restore stability in the face of swings in supply or demand, because only by reacting flexibly to constantly changing conditions – fluctuating electricity consumption, fluctuating electricity generation – the system is balanced. It's the change in feed-in or withdrawal in response to an external signal (price signal or activation) with the aim of providing a service in the system.

Flexibility services cover a range of services, of which four were defined as the ones that will be studied in this project (in T1.5). Section 2.3.1 presents electricity markets, Section 2.3.2 explains what local markets are, and Section 2.3.3 presents dynamic contracts. Then, Sections 2.3.4.1 and 2.3.4.2 explain explicit and implicit demand response, respectively.

2.3.1 Electricity Markets

The electricity market structure reflects the way in which the sector itself and its activities are organised. This is a result of the liberalisation process, which is a common feature in Europe, implemented through the publication of directives by the European Commission.

Electricity production activity in the market system is associated with a wholesale market, where production market agents ensure its placement. The market agents who require supplies seek to acquire electricity, either to meet the portfolio of end-costumer supplies or for self-consumption purposes. The supply activity is associated with a retail market, in which supply market agents compete with each other to ensure the supply of end consumers. The liberalisation model for the electricity sector also added organised markets, which are negotiation platforms that tend to be independent of traditional agents involved in electricity production and supply [14].

The electricity contracting involves multiple forms, from contracting for the following day (day-ahead spot market), to contracting closer to real time through the intraday market (through auctions and continuous trading), and for longer periods (forward market). Contracting can also take place bilaterally in the over-the-counter market and/or through specific legal or regulatory mechanisms [14].

As the energy system relies more and more on renewables, and more and more electrification of end consumption, the electricity system becomes more decentralised and interactive. The flexibility local markets help energy networks to monitor energy flows and create market signals to motivate changes in energy supply and demand.

A virtual power plant (VPP) consists of the integration of a group of distributed energy resource (DER) facilities managed by a single control system. Its main objective in participating in the electricity market is to fulfil the basic power generation obligation to meet the electricity demand. Which means that the VPP undertakes the responsibilities of both a power generator and an aggregator who organises the transactions among various energy resources in the market [15], [16].

To participate in a VPP, there are several requirements, that may vary depending on the VPP operator and location, such as,

1. Distributed Energy Resources – such as solar, batteries and controllable loads behind the meter can generate and/or store energy. This energy can be dispatched and managed by an aggregator to meet demand and supply needs.
2. Communication and Control – to participate in a VPP, DERs need to be able to communicate with the VPP operator or aggregator and be controlled by them. This may involve installing additional hardware or connecting to software that allows the DERs to be remotely monitored and managed.
3. Internet Connectivity – DERs must be connected to the internet so they can communicate with the VPP operator and receive signals about when to discharge or store energy.
4. Compatible technology – the DERs must have technology that is compatible with the VPP platform used by the operator (e.g. Energy Retailers or System Operators).

5. Agreements with the VPP operator – participants typically need to sign an agreement with the VPP operator that outlines the terms of their participation, such as payment rates, energy usage, and requirements for equipment installation and maintenance.

2.3.1.1 Next Kraftwerke

An example of an already implemented VPP is the one operated by Next Kraftwerke[5], which is a Germany-based company now part of Shell that works like a power plant operator. This VPP aggregates small generators and combined heat and power (CHP), commercial and industrial (C&I) flexible loads, storage, and renewables to participate in electricity markets and grid frequency control. They link their clients' power-producing and consuming units, creating a digital platform from which they can smartly distribute supply and demand, trading power for profit.

2.3.1.2 CyberGrid

CyberGrid[6] is an Austrian company that has a Flexibility Management Platform called CyberNoc that pools energy resources into a VPP, connecting flexibility providers to the various layers of the electricity markets, such as retailers, traders, prosumers, DSOs, TSOs, etc. Their VPP collects unused or not properly used flexibility and channels it to the electricity system, a function that serves the constantly growing renewable generation.

Also, in the EU-funded project TALENT[7], CyberGrid lead the development of a distributed architecture (VPP) for the management of decentralised and hybridised energy systems. Within that project, a battery digital twin integrated into the VPP was developed to monitor the battery connected to the system. The close monitoring of the battery state allowed for optimised exploitation of the available battery capacity to maximise the revenues, while also avoiding the fast aging of the battery.

2.3.2 Local Markets

A local electricity market is a market platform for trading locally generated (renewable) energy among the residential customers within a geographically and socially close community. Supply security is ensured through connections to a superimposed energy system (e.g. national grid or adjacent local markets).

2.3.2.1 Grid Operators Platform for Congestion Solutions

One example of already implemented local markets is the *Grid Operators Platform for Congestion Solutions* initiative (GOPACS[8]) in The Netherlands, possible thanks to the Dutch market-based approach to congestion management. In principle it could be replicated in all EU member states, except the ones that are limited by regulated redispatch (e.g., Germany).

In this market, when there is a congestion situation on the network side, i.e. the demand exceeds the supply, it is put into the GOPACS platform. A market message is generated indicating that there is a congestion, and the network operators wish to receive flexibility offers to resolve the situation. Here,

[5] https://www.next-kraftwerke.com
[6] https://www.cyber-grid.com
[7] https://talentproject.eu
[8] https://en.gopacs.eu

there are three congestion management products: redispatch; bid obligation contract; and through capacity limitation contract with demand.

On the redispatch, the network operators reduce demand for transmission capacity via GOPACS based on intraday bids. The network operator posts the congestion situation as an order. Participants with a connection in the congestion zone can respond by placing an order on the energy trading platform connected to GOPACS. The actions aimed at resolving the congestion must not cause problems in maintaining the balance of the electricity network at national level.

Therefore, the placement of a buy order is always combined with a sell order outside the congestion zone or vice versa. In this way, the congestion situation is resolved without disturbing the balance of the electricity grid. If the order is executed, the user will receive the requested price.

For the second product case, the bid obligation contract is an agreement between the network operator and a congestion service provider (CSP) directly. With an obligation-to-bid contract, the CSP enters into an individual agreement with its network operator. In doing so, it jointly agrees to make redispatch offers in GOPACS at the request of the network operator. The must-offer contract explicitly includes the electricity allocation number (EAN) connection(s) in the contract.

A purchase obligation contract offers more certainty to the participant and the grid operator than redispatch offers via an energy trading platform, as described above. Through this contract, the grid operator is sure that the congestion problem will be solved and the user, as a contractual partner, is sure of the conditions and fees, as these are agreed in advance.

The last congestion management product is the capacity limitation contract with demand. With this day-ahead contract, there's a contract agreement with the network operator that it will limit the requested transport capacity if it's requested. An on-demand contract also offers more security for the costumer and the network operator than intraday redispatch offers through this local market.

2.3.2.2 New Energy Market Design

Another local market is the *New Energy Market Design* (NODES[9]), established as joint venture between the Norwegian utility Agder Energi[10] and the European power exchange Nord Pool[11].

NODES operates a market platform that puts a value on flexibility, and it gives a buyer of flexibility a right to change consumption or production according to a contract. The main goal is to increase value for flexibility providers, and reduce costs for the DSO. Also, giving the opportunity to flexibility not used locally to be sold to the TSO and/or Balancing Responsible Parties (BRPs) at the transmission grid to solve imbalance issues there.

The trading timeline of this market consists of an early period of trading with capacity – or availability products. This normally lasts from years ahead and until the opening of the day-ahead auction. The intraday market in most European countries starts after the day-ahead market has closed. Here the BRPs can rebalance their portfolio continuously until gate closure (60 to 0 minutes before operating period depending on country). The TSO has several products outside the current intraday market which they can use to manage congestions.

[9] https://nodesmarket.com
[10] https://www.aenergi.no/en
[11] https://www.nordpoolgroup.com

NODES enables DSOs to model congested grid areas and publish them as local markets in the NODES market platform. When a local market is created, suppliers of flexibility can register their flexible assets and offer ramp down and ramp up of consumption or production to the DSO to alleviate local bottleneck.

Aggregators, power suppliers or technology companies who can control consumption or production units can sell consumption/production ramp up or ramp down to local DSOs.

2.3.2.3 Piclo Flex

Created by Piclo, a UK based company, that develops software solutions, Piclo Flex[12], is an independent marketplace for energy flexibility services, enabling system operators to source energy flexibility from flexible service providers (e.g. electric vehicles) during times of high demand or low supply, by simplifying the process from flexibility service providers (FSPs) to DSOs.

The FSPs can upload assets, qualify them, and bid for flexibility contracts advertised by DSOs on Piclo Flex. The DSO receives these bids from qualified FSP and will either accept or reject them based on considerations such as price. If the bid is accepted, the DSO and the FSP enter into a Flexibility Services Agreement, where the DSO will send despatch instructions to make payments to the FSP.

With this, the FSPs can optimise the use of their assets and earn additional revenue streams, with contracts extending up to 7 years providing long term income opportunities.

This platform is currently available in Great Britain, Italy, Ireland, the United States, and Portugal.

2.3.3 Dynamic Contracts

In a dynamic power contract, also called capacity limitation contract, a portfolio of flexible consumers or prosumers enters an agreement with the system operator to limit the contracted power, when requested, in exchange for a payment or benefit [17]. Normally, this type of contracts is established when the installed power is higher than the grid capacity. The main advantage is to reduce the need of investments in the grid that normally should be supported by the consumers/producers.

This type of services is used, normally, for distributed generation, as reported in [18]. However, considering the high-power demand imposed by charging stations, it is expected that new type of dynamic contracts can be proposed smoothing the investments in the grid [19].

To enable this kind of contracts a close coordination between the system operators and the consumers/producers is mandatory. Another important aspect is the use of intelligent control strategies and systems to guarantee that the limits requested by the system operators are respected. In the specific case of electric vehicles this can be ensured by EVs management systems, as the one proposed in deliverable D1.6 [20] or can be managed directly in the house/building energy management system. In both cases, the power consumption during the limitation periods will impose some limitation in the charging of the EVs or, if possible, the use of V2X capability to compensate it.

2.3.4 Demand Response (DR)

DR is a technique that opens the electricity market to consumer participation by decreasing peak loads or adjusting energy usage in response to dynamic pricing. This technique can reduce costumers'

[12] https://picloflex.com

electric bill costs and decrease peak demand. It also provides insurance against volatility of real-time market prices and helps to mitigate risks associated with unpredictable pricing for energy providers [21].

There are two classes of DR: implicit demand response, also called Price-Based Demand Response (PBDR), and explicit demand response, also called incentive-based demand response (IBDR). PBDR programs use pricing signals such as time-of-use (ToU) pricing, critical peak pricing (CPP), and real-time pricing (RTP) to encourage customers to manage their electricity usage. In contrast, IBDR programs provide customers with monetary rewards or penalties for decreasing their electricity usage at peak times [21].

A DR is, then, a programme established to encourage changes in the consumption patterns of final consumers. This is done in response to changes in the price of electricity, the price of electricity over time, incentives, or when the reliability of the grid is called into question.

DR has already been playing an active role in the electricity system for years, for instance, retailers offer ToU prices to their consumers in several countries (e.g. Portugal). There are also many costumers that participate in explicit demand response through an aggregator and, at the same time, participate in an implicit demand response programme through dynamic tariffs. Consumers receive a lower bill for participating in a dynamic tariff programme and will receive a direct payment for participating in an explicit demand response programme. Nevertheless, it is important to mention that dynamic pricing also present a higher risk due to market price fluctuations.

2.3.4.1 Explicit-Based Demand Response

In explicit demand response the result of demand response actions is sold upfront on electricity markets, sometimes directly for large industrial consumers or through curtailment service providers. Then, the consumers receive a specific reward to change their consumption upon request, triggered by high electricity prices, flexibility needs of balance responsible parties or a constraint on the grid.

The Italian company EnelX[13] manages explicit demand response services in several countries in the world, such as Italy, Poland, the United Kingdom, the United States, and South Korea. Their programs are opened to all enterprises with at least 100 kW of connected power, and which can, for a short time:

- Shift the power consumption to other hours;
- Temporary reduce power consumption;
- Switch to a back-up generation source or energy storage.

In the state of New York in the United States, *New York Independent System Operator* (NYISO) has in place two explicit demand response programs, also called reliability-based demand response programs. The objective of these is to pay the consumer for load reduction when the electrical grid is stressed, such as when demand for electricity is above the normal levels (peak periods), or there are unplanned events like extreme heat, inclement weather, or transmission outages. These two programs are called Installed Capacity – Special Case Resource (ICAP-SCR) program and the Emergency Demand Response Program (EDRP) [22].

For these programs, the NYISO usually sends notifications both a day before the vent, and on the day of the event (typically two hours prior to the load reduction period). As an ICAP-SCR participant,

[13] https://www.enelx.com

performance is mandatory when both the day-ahead and two-hour notifications occur, at which the consumer is obligated to reduce load for a minimum of four hours during the event. The same applies for the EDRP program; however, performing the load reduction during any event is voluntary [22].

2.3.4.2 Implicit-Based Demand Response

Implicit demand response refers to consumers who choose to be exposed to time-varying electricity prices that reflect the value and cost of electricity in different time periods. With this, consumers can decide to shift their electricity consumption away from times of high prices or grid constraints, and thereby reduce their electricity bill. Time-varying prices are offered by electricity suppliers and can range from simple day and night prices to highly dynamic prices based on hourly wholesale prices. As mentioned earlier, this includes time-of-use pricing, critical peak pricing, and real-time pricing.

In ToU pricing, there is time-based electricity billing, where costumers are billed based on the cost per kilowatt-hour, determined by the specific time of their energy consumption. By dividing the day into predefined periods such as day and night, on-peak and off-peak, costumers have the opportunity to take advantage of the prevailing consumption patterns and unlock potential savings. This is currently implemented in Portugal, Denmark, and Greece [23].

In Portugal the time-of-use pricing is divided into three tariffs: simple tariff, bi-hourly tariff, and three-hourly tariff. In the simple tariff the consumer pays electricity at the same price for all hours of the day. In the bi-hourly tariff, the consumer pays electricity at two different prices, for two corresponding hourly consumption periods: the empty hour period, in which the energy has a lower cost; and the period of hours of outside of empty, in which the energy has a higher cost [24].

The three-hourly tariff is similar to the two-hourly one, but it has three hourly consumption periods with different prices: the valley period, the normal period, in which the energy has an intermediate cost, and the peak period, in which energy has a higher cost [24].

CPP operates as a ToU plan, incorporating an additional top-up rate for select days when electricity prices significantly exceed the average. This approach aims to alleviate load during limited but high-cost hours. Key components of this pricing plan include the defined time window during the peak price period and the degree of price differentiation between peak and off-peak times.

Southern California Edison's (SCE) in the United States uses CPP as the default option for small, medium, and large business customers, as well as large Agricultural and Pumping ones. It provides four months of summer season bill credits in exchange for paying higher electricity prices during 12 to 15 annual CPP events. When called, CPP events are from 4 p.m. to 9 p.m., usually occurring on the hottest summer days. If the company reduces its electricity use when it's notified of CPP events, it can minimize those higher prices. It will also earn credits on its electricity bills during the summer season [25].

When it comes to the RTP plan, the calculation of costumer bills is based on real-time consumption readings captured at least hourly by smart meters. As a result, suppliers operate on a small but fixed margin for every unit of electricity delivered. This pricing plan in currently implemented in Slovenia, and Portugal [23], [26].

Southern California Edison also has a RTP program designed for costumer operations with the flexibility to shift or reduce electrical usage to help bring down their energy costs. This program has energy charges, where the cost per kilowatt-hour of energy used varies each hour based on the following factors [27]:

- Time of day – where the rates are generally higher in the evening than morning or afternoon.

- Time of year – divided into two seasons. The summer season, beginning June 1 and continuing through September 30, and the winter season from October 1 to May 31.
- Weekday or weekend – holidays observed on Mondays are billed at the weekend rates, depending on the temperature.
- Daily maximum temperature – temperatures are based on the previous day's high temperature.

NYISO also has two implicit demand response programs, or economic-based demand response programs, where they give the consumer the opportunity to offer load reduction in New York's electricity markets at any time, regardless of a reliability need. These programs are called Day-Ahead Demand Response Program (DADRP), and the Demand-Side Ancillary Services Program (DSASP) [22].

When the consumer participates in the DADRP and has its reduction offer accepted and scheduled, and then receives performance payments based upon the amount of reduction made during that period. As a DSASP participant, the consumer is eligible to receive payments from the ancillary services market when the reserves and/or regulation offers are accepted [22].

3 Battery Degradation Mechanisms

To elucidate the characteristics of battery degradation, this chapter will describe the prominent degradation effects observed in a lithium-ion battery, along with the two primary aging mechanisms responsible, while delineating the key factors influencing them.

Moreover, this study does not aim to encompass all the relevant electrochemical, particle, and physics theory. Instead, it concentrates on the most significant degradation mechanisms and their consequential effects, essential for comprehending the battery's lifespan degradation when delivering various V2X services.

First, in Section 3.1, a presentation of the main degradation effects is performed. In Section 3.2, the calendar aging mechanism is explained, which includes all the aging processes that lead to the degradation of a battery regardless of the charge-discharge cycle, i.e., the degradation in battery performance during storage. Finally, in Section 3.3, the cycle aging mechanism is explained, which occurs when the battery is in use and depends on the frequency of the charge-discharge cycles [28], [29].

3.1 Main Degradation Effects

There are two prominent metrics that are used to assess the level of battery degradation: capacity fade and power fade. Capacity fade refers to the reduction in the capacity of a cell/pack to store energy caused by its degradation. It emerges as a gradual decline in the amount of battery capacity that can be charged/discharged throughout the life of a battery [30].

The power fade is defined as the decrease in the power of a cell/pack due to an increase in cell resistance. It is the gradual reduction in a battery's power capacity by a steady increase in the battery's cell impedance over time [30].

From the initial charge of a battery, the lithium ions react with the solvents of the electrolyte to form a passivation layer known as the solid electrolyte interphase (SEI) which forms on the anode, that plays an important role in the degradation of a battery [30].

The capacity fade of a battery is caused mainly by the growth of this SEI layer on the anode, through the consumption of cyclable lithium during the growth of the passivating layer. This effect, combined with the changes in porosity of the materials, also contributes to the capacity fade, where these types of changes are negligible during the early cycles of the battery operation [31], [32].

The growth of the SEI layer also causes power to fade through an increase in the resistance of the film growth [31].

When it comes to the battery impedance, it changes gradually with repeated cycling over its lifetime. Due to the accumulation of the SEI layer on the anode surface, the charge transfer resistance of the battery increases gradually, thereby increasing its overall impedance, which contributes to the power fade [33].

Figure 3.1 presents a resume of the different phases of battery degradation during its lifetime.

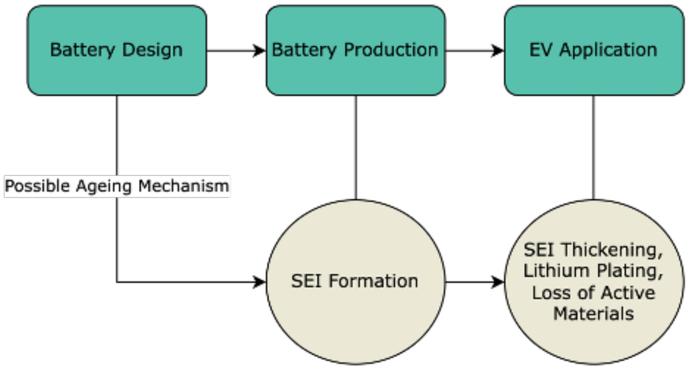

Figure 3.1: Different phases of battery degradation during its lifetime based on [30].

Knowing what the main effects of degradation are, it is then important to focus on the main factors that affect the battery life, which include [28]:

- High temperature;
- Low temperature;
- High state-of-charge;
- Low state-of-charge;
- High charge/discharge rate.

These factors have a different impact depending on whether the battery is in storage or cycling.

3.2 Calendar Aging Effects

This mechanism starts immediately after a battery is produced and increases over time. It is usually considered that the calendar life is the time for which the battery can be stored as inactive until its capacity degrades to 80% of its initial capacity [28], [29].

During storage, the main factors that affect the battery capacity are the temperature and the state-of-charge at which the battery is when it's in storage mode [34].

3.2.1 Temperature

When the battery is charging or discharging (can be called storage mode), high ambient temperatures influence the battery electrolyte and solid phase diffusivity and change the exchange current density considerably. This increases the internal resistance of the battery and therefore reduces the battery capacity, contributing to accelerated aging [32], [34].

3.2.2 State-of-Charge (SoC)

The SoC of a battery can be described as the level of charge relative to its capacity. The units are percentage points and can be defined by,

$$SoC(t) = \frac{Q_{remaining}(t)}{Q_{max}(t)} \times 100\ [\%] \tag{1}$$

where $Q_{remaining}(t)$ is the remaining capacity of the battery at a given time t and $Q_{max}(t)$ is the maximum capacity of the battery.

It is known that the open-circuit voltage increases with the SoC. During storage, the higher the SoC, the higher the open-circuit voltage, V_{OC}. However, high V_{OC} causes loss of capacity and increases the internal resistance of the battery. On the other side, a SoC lower than a certain level also increases the internal resistance. This means that if a battery is kept in an intermediate SoC when not cycling, it can reduce the battery degradation and extend battery life. It's usually recommended to charge or discharge the battery before storage to have it with a SoC equal to 50% [34].

3.3 Cycle Aging Effects

This mechanism happens during the charge and discharge of a battery. The main factors that affect the battery's capacity during cycling are the temperature (Section 3.3.1), charge and discharge rates (Section 3.3.2), the charge voltage (Section 3.3.3), depth-of-discharge (Section 3.3.4), cycle frequency (Section 3.3.5), and the state-of-charge (Section 3.3.6).

3.3.1 Temperature

When it comes to the effect of the ambient temperature on the battery life during cycling it can be as what happens in the calendar aging. An increase in the temperature during battery operation can improve performance, but over a certain limit can have the opposite effect. For example, there are manufacturers who specify the nominal temperature of 27 °C to extend he battery's operation, but prolonged cycled at high temperatures reduce battery life. A battery operated at 30 °C has a life cycle reduced by 20%. At 45 °C, the battery only has half of its optimum life, which can be achieved when operated at 20 °C [34].

At low temperatures, the limitation on the diffusion of lithium ions into the SEI layer and the electrodes leads to another phenomena called lithium plating and lithium dendrite growth. In particular, lithium plating occurs at a low temperature during the charge of a battery [35].

Whether with high or low temperatures, there's always an increase in the internal resistance, which decreases a significant amount of discharge capacity [34].

When it comes to the internal temperature of a battery, the main contributions to the heat generation inside a battery are from ohmic heat generation and reaction heat generation, and comparatively less from reversible heat. The ohmic heat is due to the limited internal conductivity, and this term accounts for the ohmic heat in the solid phase as well as the electrolyte phase. There is a sharp increase in temperature during the initial phase of the charge cycle, and subsequently the battery reaches a balance between the internal heat generation and the heat convected outside. There's a small decrease in temperature when the battery changes from a charge cycle to a discharge cycle [32].

3.3.2 Charge/Discharge Rates

A battery's charge and discharge rates are represented by battery C-rates. It is a representation of a charge and discharge current normalized to battery capacity. The capacity of a battery is generally rated and labelled at the 1C, which means that a fully charged battery with a capacity of 10 Ah should be able to provide 10 A for one hour. If the same 10 Ah battery is being discharged at a C-rate of 0.5C it will provide 5 A over two hours, and if discharged at 2C it will provide 20 A for 30 minutes. This measure is important to know that the available stored energy depends on the speed of the charge and discharge currents.

When it comes to battery degradation, high load currents, i.e. high C-rates, cause an increase in the internal resistance of the battery and increase the loss of capacity. They also cause greater energy loss because part of the energy is transferred by heat due to the internal resistance [34], [36], [37].

At low C-rates, such as 0.1C, the performance of the cell and pack are reasonably consistent, however when C-rates are increased to 1.5C the variation in cell voltage is more substantial. This variation between single cell and pack performance can be attributed to the interconnect resistances, which can cause uneven current distributions [31].

3.3.3 Charge Voltage

The charge voltage of a battery is the amount of battery voltage when the battery is fully charged, or the voltage available at any given point during the charging process.

A high charge voltage gives high capacity and allows the battery to last longer. However, it is not recommended to fully charge the batteries. For example, charging above 4.1 V/cell with nominal voltage of 3.9 V, not only reduces the battery's capacity, but it can also lead to internal short-circuiting. Then, high charging cut-off voltages accelerate the aging phenomena, particularly the capacity fade. Whereas low discharging cut-off voltages affect the aging, particularly the power fade [34], [35].

3.3.4 Depth-of-Discharge (DoD)

DoD is the fraction or percentage of the battery's capacity which is currently removed from the battery, regarding its (fully) charged state. For fully charged batteries, the depth of discharge is connected to the SoC by,

$$DoD(t) = 100\% - SoC(t) \tag{2}$$

The DoD then is the complement of the SoC, as one increases, the other decreases.

A DoD above 80% is considered a deep discharge, which accelerates the capacity loss because the higher the DoD cycle, the shorter the battery's cycle life. It is therefore advised to avoid a complete discharge during the cycle [34].

Due to that, battery's manufacturers normally use the formula 80% of DoD, which means that only 80% of the input energy is delivered during battery use and the other 20% is reserved to achieve a longer battery service life [34].

However, although lower DoD extends the battery life cycle, if it's too low it can lead to insufficient battery life and the inability to complete certain tasks. A DoD of 50% is recommended when using batteries, to achieve maximum life, such as providing optimum service time [34].

3.3.5 Cycle Frequency

A discharge/charge cycle is the complete discharge of a charged battery followed by a recharge [28]. Then, the cycle frequency is defined as the number of cycles a battery performs in, for example, a day. In the event of a high frequency of cycles (for example, several per day), there is a decrease in both battery capacity and charging efficiency [34].

Frequent cycles without a break in between adds stress to batteries, partly due to the increase in cell/pack temperature during cycles and the lack of time for cooling. Thus, under the same cycling environment (i.e. temperature, current, voltage, etc.), batteries that have more rest time during cycles have a longer cycle life [34]. This is the number of complete cycles it can be charged and discharged before its capacity degraded to 80% of its initial capacity [28].

3.3.6 State-of-Charge (SoC)

As mentioned in Section 3.2.2, a higher SoC indicates a higher terminal voltage. High SoC levels correspond to high concentration of ions on the electrodes. Therefore, a large potential difference between the electrodes and the electrolyte interfaces leads to chemical reactions, which age the battery. When it comes to low state-of-charge levels they also cause an increased aging, due to the corrosion of the materials [28], [34], [35].

For example, due to state-of-charge effects, a cycle from 100%-80% of SoC will not result in the same degradation as a cycle from 40%-20% of SoC, although they would both constitute a DoD equal to 20%.

4 Battery Degradation Modelling

Truly empirical lifetime analyses would require time scopes of several years or more, which is both impractical and would be rendered obsolete at completion, as battery technology is improving rapidly. Due to these challenges, semi-empirical electrochemical models have been developed that aim to model fundamental electrochemical phenomena mathematically while extracting rate relationships from the limited degradation data available [38, p. 2], [39], [40].

Since the purpose of this work is to perform a characterization of lithium-ion batteries degradation considering the participation in V2X services, it was necessary to then be able to simulate the battery degradation in each of the use-cases explained in Chapter 2. To do this, there was a need to find a semi-empirical electrochemical and combined electrochemical-thermal lifetime model that could be used to evaluate both calendar and cycle aging, instead of the other modelling methods such as equivalent circuit models, reduced order models, statistical methods, and other methodologies that have been covered in previous review articles, that are mainly used to characterize battery operational behaviours, instead of battery lifetime degradation.

Also, it needs to be a mathematical model where several variables could be changed to fit each service and condition of simulation. Finally, it was necessary to also be able to be incorporated into already existed tools that allow to simulate lithium-ion batteries in various conditions.

To find the most suited model, extended research was performed, and the three main models found are presented in the following sections. Section 4.1 presents the *National Renewable Energy Laboratory* (NREL) model, Section 4.2 the *Modelling of Batteries Including the coupling between Calendar and Usage aging* (MOCIBUS), Section 4.3 the Wang model. In the end, Section 4.4 presents the comparison between the three models and what model was chosen.

4.1 NREL Model

The NREL model was originally based upon a lithium nickel cobalt aluminium oxides (NCA) chemistry dataset, which was later updated to incorporate a lithium iron phosphate (LFP) chemistry [39], [41]. This model assumes that the fundamental degradation behaviour is similar for all the lithium-ion technologies but has degradation coefficients that depend on the chemistry. Its main outputs are battery capacity and internal resistance, and both calendar aging and cycle aging are incorporated.

The cell capacity is defined by the minimum of the capacity loss attributed to the loss of active lithium material (Q_{li}) in contrast to the loss of active sites (Q_{sites}) in the electrolyte of the cell, given by [5],

$$Q = \min(Q_{li}, Q_{sites}) \tag{3}$$

where,

$$Q_{li} = b_0 + b_1 t^z + \cdots \tag{4}$$

$$Q_{sites} = c_0 + c_1 N + \cdots \tag{5}$$

Also, b_1 is the rate constant for the time effect on lithium loss, and c_1 is the constant for the cycle number effect on site loss.

The internal resistance is defined as [5],

$$R = a_0 + a_1 t^{1/2} + a_2 N \tag{6}$$

where a_1 is the rate constant for the time effect on resistance, and a_2 is the cycle number effect on the resistance.

The model coefficients are developed from generalized rate constants equations that assume an Arrhenius[14] dependence on temperature (θ_T), a Tafel[15] dependence on open-circuit voltage (θ_{VOC}, which, as was previously mentioned in Chapter 3 is related to the state-of-charge), and a Wöhler[16] dependence on changes in depth-of-discharge (θ_{DoD}) [42], [43], [44].

These dependences are defined by the following equations [5],

$$q_T = exp\left[\frac{-E}{R}\left(\frac{1}{T(t)} - \frac{1}{T_{ref}}\right)\right] \tag{7}$$

$$q_{VOC} = exp\left[\frac{aF}{R}\left(\frac{V_{OC}(t)}{T(t)} - \frac{V_{ref}}{T_{ref}}\right)\right] \tag{8}$$

$$q_{DoD} = \left(\frac{D\ DoD}{D\ DoD_{ref}}\right)^b \tag{9}$$

where E, α, β and θ_{ref} are fitting parameters that depend on the chemistry specific behaviour. R is the universal gas constant and F is the Faraday constant. The reference parameters are chosen to normalize aging to standard conditions and are defined as presented in Table 4.1.

Table 4.1: Parameter values and units for the reference parameters of Equations (7)-(9).

Parameter	Value	Unit
T_{ref}	298.15	K
V_{ref}	3.6	V
ΔDoD_{ref}	1	*Unitless*

To resume, this model predicts incremental aging over an assumed standard aging profile.

4.2 MOCIBUS Model

The MOCIBUS models are a product of research projects since 2007. The two models are based on two different projects, one for cycle aging and another for calendar aging [39].

4.2.1 Cycle Aging Model

This model comes from the SIMSTOCK project for an lithium manganese oxide + lithium nickel manganese cobalt oxide (LMO-NMC) blend battery chemistry and was initially formulated as a polynomial expression [45],

$$F(Y) = y_{00} + y_{01}X_1 + y_{02}X_2 + y_{03}X_3 + y_{04}X_4 \tag{10}$$

[14] The Arrhenius equation is a formula for the temperature dependence of reaction rates.
[15] The Tafel equation is an equation in electrochemical kinetics relating the rate of an electrochemical reaction to the overpotential.
[16] The Wöhler dependence is a curve that relates the number of cycles with the depth-of-discharge.

where X_1 is the current, X_2 is the temperature in degrees Celsius, X_3 is the current throughput in A/s and X_4 is the state-of-charge variation ($DSoC$). The variable Y represents the total aging, considered as cumulative Ampere-hours.

The aging parameters are considered static throughout the life of the battery cell, which is a limitation as the rates at which degradation parameters affect the overall battery life fade will change as the battery ages. Therefore, to capture the changes in the degradation rate losses, the model was adapted to calculate the differential capacity loss and was formulated as [39],

$$\left(\frac{d_{Q_{Li}}}{d\left(\sqrt{t}\right)}\right) = a_j \tag{11}$$

where,

$$a_j = a_{00} + a_{01}X_1 + a_{02}X_2 + a_{03}X_3 + a_{04}X_4 \tag{12}$$

As this model is in derivative form, it attempts to predict the instantaneous rate at which the capacity declines during each battery test condition, then integrates each individual slope over time to result in the full capacity degradation.

4.2.2 Calendar Aging Model

This model was presented for an LFP battery chemistry, which was subjected to six storage conditions for a total of 14 tests. Batteries were stored at state-of-charges of 30%, 65% and 100% while being subjected to temperatures of 30 °C, 45 °C, 60 °C, and a thermal cycling test which varied temperature from 30 to 45 °C. This model was also initially formulated as a derivative equation [5],

$$\frac{dQ_{loss}}{dt} = k(T, SoC)\left(1 + \frac{Q_{loss}(t)}{C_{nom}}\right)^{a(T)} \tag{13}$$

where $k(T, SoC)$ is the kinetic dependence of capacity fade evolution with temperature and state-of-charge during storage, $Q_{loss}(t)$ divided by C_{nom} is the fractional capacity loss at time t, and $(1 + Q_{loss}(t)\ /\ C_{nom})^{-a(T)}$ with $a(T) < 0$ is related to the diffusion limitation of solvent molecules inside the SEI layer which tends to decrease the capacity fade rate and depends on the temperature.

To express the total capacity loss as a function of time, the incremental representation seen in Equation (13) was integrated by making $\alpha = 1$ at $t = 0$ for $Q_{loss} = 0$, which resulted in [5],

$$k(T, SoC) \times t = Q_{loss}(t) + \frac{1}{2}\frac{Q_{loss}(t)^2}{C_{nom}} \tag{14}$$

To better fit the aging dataset, the model was further generalized to allow for model tuning to aging data that didn't follow an Arrhenius evolution. This was accomplished by integrating the Equation (14) and assuming the temperature and state-of-charge to remain constant to result in the following equation [5],

$$t = \frac{C_{nom}}{(a+1) \times k(T, SoC)}\left\{\left(1 + \frac{Q_{loss}}{C_{nom}}\right)^{a+1} - 1\right\} \tag{15}$$

where,

$$A(T) = k_a \times exp\left\{-\frac{Ea_A}{R}\left(\frac{1}{T} - \frac{1}{T_{ref}}\right)\right\} \tag{16}$$

$$A(T) = k_a \times exp\left\{-\frac{Ea_A}{R}\left(\frac{1}{T} - \frac{1}{T_{ref}}\right)\right\} \tag{16}$$

$$B(T) = k_b \times exp\left\{-\frac{Ea_B}{R}\left(\frac{1}{T} - \frac{1}{T_{ref}}\right)\right\} \tag{17}$$

In these equations, the model parameters α and k were estimated through non-linear regression techniques to fit the baseline model to the aging data.

4.3 Wang Model

The Wang model is based upon accelerated life testing of a large test matrix of battery conditions of the 1.5 Ah 18560 LMO-NMC Sanyo technology, which drew upon previous work that modelled cycle life of LFP cells. This study provided a thorough description of both the test conditions and the measurement techniques employed to characterize the batteries. The cells were characterized by four techniques: capacity characterization, relaxation tests, electrochemical impedance spectroscopy (EIS), and hybrid pulse power characterization (HPPC). Additionally, this study conducted a voltage differential analysis to examine the source of capacity loss and concluded that lithium loss was the limiting factor thus the active site loss wasn't modelled as in the NREL model [38], [46].

This model defined two models, one for calendar aging, and another for cycle aging.

4.3.1 Calendar Aging Model

The calendar aging model was developed from fitting model parameters to have a capacity loss equation which assumed an Arrhenius dependence on temperature. Thus, the calendar aging was defined as [5], [47], [48],

$$Q_{calendar,\%} = A \times exp\left(-\frac{E_a}{RT}\right) t^{1/2} \tag{18}$$

where, A is a pre-exponential factor, E_a is the activation energy, R is the gas constant, T is the average temperature, and t is the total lifetime of the battery cell.

4.3.2 Cycle Aging Model

The degradation due to cycling was calculated by subtracting the calendar aging model from the total loss measured from the data, thus obtaining a cycle aging equation hypothesized from the rate effect of the C-rate given by [5],

$$Q_{cycle,\%} = B_1 \times \exp(B_2 \times \ rate) \times \ Ah_{throughput} \tag{19}$$

where B_1 is the pre-exponential fitting factor, and B_2 an exponential fitting factor.

A generalized equation to take all the temperatures and rates into account was found by an empirical fitting of B_1 and B_2 factors of the cycle aging model, described as [5], [47], [48],

$$Q_{cycle,\%} = (aT^2 + bT + c) \times \ exp[(dT + e) \times \ C_{rate}] \times \ Ah_{throughput} \tag{20}$$

where T is the average temperature of the cell, C_{rate} is the average C-rate, $Ah_{throughput}$ is the average throughput of energy, and a, b, c, d, and e are pre-defined factors.

All the coefficient values and units for both the calendar and cycle aging models are presented in Table 4.2, where C_{rate} is unitless.

Table 4.2: Coefficient values and units for calendar and aging models.

Coefficient	Value	Unit
a	$8.610 \cdot 10^{-6}$	$1/(Ah \cdot K^2)$
b	$5.130 \cdot 10^{-3}$	$1/(Ah \cdot K)$
c	0.760	$1/(Ah)$
d	$6.70 \cdot 10^{-3}$	$1/(K \cdot s)$
e	2.340	s
t	-	days
E_a	24.500	kJ/mol
R	8.314	$J/(mol \cdot K)$
T	20.000	°C
A	14.876	$days^{-1/2}$

4.3.3 State-of-Health

Based on the equations presented for the calendar and cycle aging models, it's then possible to compute the actual battery capacity by,

$$Q(t) = Q_{nom}(t) \times \left(100\% - Q_{calendar,\%}(t) - Q_{cycle,\%}(t)\right) \tag{21}$$

and the state-of-health of the model given by,

$$SoH_{model,\%}(t) = 100\% - Q_{calendar,\%}(t) - Q_{cycle,\%}(t) \tag{22}$$

4.4 Models' Comparison

Before comparing the three presented models and deciding what best suited the needs of this task, it is important to understand the difficulties found with these types of models.

While semi-empirical battery models are the most adequate tools for predictive analysis due to the cost prohibitive elements of empirical full life cycle testing, they are inherently limited by their source data, both in the test conditions and in the characteristics of the cells that were studied. This limitation is manifested in several ways:

1. **Time resolution**: current models do not consider micro cycling (defined as rapid changes of the battery current direction between charging and discharging), and calculate degradation by temperature from average impact, normally at an hourly timeframe.
2. **Data limitation**: It is difficult to predict beyond 10 years and below a capacity fade of 30% as no empirical dataset has yet been generated, and there's also a lack of data at extreme temperatures. Additionally, cell-to-pack translations of aging data are known to produce biased results. This is due to cell-to-cell variations within the battery pack, which produce temperature non-uniformities and thus non-uniform aging.

3. **Lack of test cycle standardization**: Cycle definitions should include charge rate, temperature (both ambient and effective cycle temperature), a well-documented charge profile, a clear definition of what a cycle constitutes, and acknowledgement of rest times between cycles or between measurements. A clear definition of battery measurement and characterization techniques (EIS, charge/discharge, HPPC, etc.) should also be provided.
4. **Chemistry limitation**: Different Lithium-Ion chemistries have drastically different aging profiles, thus the need to expand current models to additional chemistries is clear.

Having these limitations in mind, it is then possible to compare the models. While the NREL model seems the most well-developed, it is limited to two chemistries and is based on population data primarily from geosynchronous orbit satellite life qualification tests.

The MOCIBUS project has access to the most robust aging data set from the greatest variety of battery chemistries. However, the overall modelling approach to couple calendar and cycle aging isn't clear, as there are no known published works yet. Therefore, model dependencies must be inferred from previous models developed out of the research of the SIMSTOCK[17] and SIMCAL[18] projects.

The Wang model is also well-developed, with additional insights related to which degradation mechanisms bound capacity loss and the visualization of the calendar vs. cycle aging effects. However, this model is limited to the NMC-LMO chemistry and doesn't employ actual storage data as it assumes a low C-rate, low depth-of-discharge cycling data would be comparable.

As mentioned in the beginning of this chapter, for the objective of the task, it was necessary to find a model that had, preferably, two different mathematical equations. One for calendar aging and another for cycle aging, due to these being the main degradation mechanisms and affected by different factors. Also, the model needed to have the ability to be incorporated into software tools that could simulate the degradation in several grid services. For this, the Wang model is the most adequate. It was found to be the model that is most used in literature, due to also being able to have a good compromise between the degradation of a cell and the degradation of a pack.

[17] https://ieeexplore.ieee.org/document/6043110
[18] https://trimis.ec.europa.eu/project/study-and-modeling-calendar-aging-nimh-and-li-ion-batteries-embedded-road-vehicles

5 V2X Services' Battery Degradation Simulations

To simulate the degradation of a lithium-ion battery in each of the V2X Services mentioned in the Chapter 2, it was necessary to find a library, preferably open-source, that allowed the integration of the model chosen in Chapter 4. It should then include the characteristics of each of the services and simulate several scenarios to understand how, in theory, the batteries would age.

For this, a Python library named PyBaMM[19] was used. It is an open-source battery simulation package that consists of a framework for writing and solving systems of differential equations, a library of battery models and parameters, and specialized tools for simulations of battery-specific experiments and visualizing the results. This tool focus on the cell-level, allowing to simulate one battery with a defined number of cells connected in series.

For the simulations, the flexibility services (electricity and local markets, dynamic contracts, implicit and explicit demand response) were aggregated, due to the demand on a battery in V2X context being the same in all these services.

In these simulations, the parameters for the EV battery and the chosen ambient conditions are presented in Table 5.1, and were included in the model presented in Chapter 4.

Table 5.1: EV Battery parameters considered in the performed simulations.

Parameter	Value
Battery nominal capacity [Ah]	176.4
Battery nominal voltage [V]	350.4
Battery nominal energy [kWh]	61.8
Initial State-of-Charge [%]	50.0
C-rate	1

In order to simulate the services, the PyBaMM python library requires commands to be sent in a certain format in what it's called an "Experiment". For example, when we want the battery to be at rest mode a certain period, the command can be written as "Rest 1C for 15 seconds". If we want to charge the battery at 1C (C-rate equals 1) for one minute, the command would be "Charge at 1C for 1 minute", and if instead we wanted to discharge it would be "Discharge at 1C for 1 minute". It is also possible to limit until it reaches a certain voltage, for example, "Charge at 1C for 30 seconds or until 4.2 V".

With this, Section 5.1 presents the results of the simulations performed for wind curtailment, Section 5.2 for frequency regulation, and Section 5.3 for the flexibility services.

[19] https://pybamm.org

5.1 Wind Curtailment Service

For wind curtailment service, we used the data mentioned in Section 2.1.1 for the island of São Miguel in the Azores. In this case, when there's a need to curtail wind, we want to charge the battery with that energy avoiding curtailment. Because it would've been only charge or rest mode it was decided to consider a discharge of 10 kWh at 1C per day.

To better understand the demands of this service, Table 5.2 shows the maximum time in each of the analysed months that the EV battery would be in rest and charge modes considering the number of times there was wind curtailment and the duration of that event. Here, in a whole month the service would require for a battery to be charging almost uninterruptedly, because even though the highest curtailment occurs during the night, there's also curtail during the day.

Table 5.2: Maximum time the EV is in rest and charge modes when considering the wind curtailment in the São Miguel Island.

Month-Year	Maximum time in rest mode [days]	Maximum time in charge mode [days]
Jan-22	3.9	9
Feb-22	0.2	6
Mar-22	0.5	18
Apr-22	0.1	10
May-22	0.4	10
Jun-22	1.2	13
Jul-22	0.8	11
Aug-22	0.5	12
Sep-22	0.6	18
Oct-22	0.4	16
Nov-22	0.4	5
Dec-22	0.5	10

Table 5.3 shows the total time in each of the analysed months that the EV battery would be in rest and charge mode considering the wind curtailment in São Miguel. In this case, in a whole month the service would require the battery to charge the equivalent to almost every day.

Table 5.3: Total time the EV battery is in rest, charge, and discharge modes when considering the wind curtailment in São Miguel Island.

Month-Year	Total time in rest mode [days]	Total time in charge mode [days]
Jan-22	5	26
Feb-22	1	27
Mar-22	1	30
Apr-22	1	29
May-22	3	28
Jun-22	5	25
Jul-22	4	27
Aug-22	5	26
Sep-22	2	28
Oct-22	2	29
Nov-22	2	28
Dec-22	1	30

From Table 5.2 and Table 5.3 it can be observed that this service would have a high demand for an EV battery due to the elevated need to charge (and then discharge), i.e. there would be a high cycle aging when compared to the calendar one.

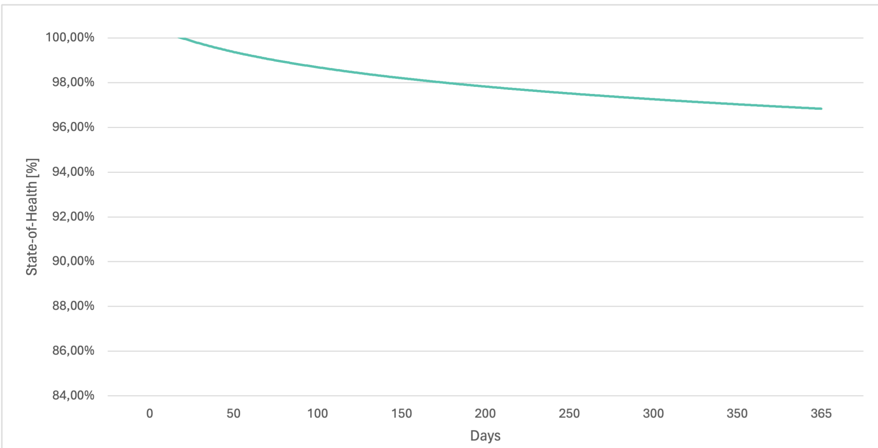

Figure 5.1 presents the state-of-health obtained from the simulations with the data from January 2022 to December 2022, respectively.

Figure 5.1: Battery State-of-Health considering the EV participation in Azores wind curtailment data from January 2022 to December 2022.

It can be observed that in this service, in 12 months there would be a loss in state-of-health of almost 4% in a year.

5.2 Frequency Regulation

For the frequency regulation services the simulations were divided into two main ones. First, considering the data from the Continental synchronous area. Second, considering the data from the Nordic synchronous area.

5.2.1 Continental Synchronous Area

The simulations considering the data from the continental synchronous area were separated into the frequency deviations that occur outside of the so-called normal frequency range, i.e. between 49.9 Hz and 50.1 Hz, and the deviations outside of the nominal frequency, 50 Hz.

Table 5.4 presents the maximum time the EV would be in rest, charge, and discharge modes when considering the deviations outside the interval [49.9; 50.1] Hz for this area. It is perceivable that the maximum required charge/discharge time for the service would be approximately 5/6 minutes.

Table 5.4: Maximum time the EV is in rest, charge, and discharge modes when considering the deviations outside the interval [49.9; 50.1] Hz for the Continental synchronous area.

Month-Year	Maximum time in rest mode [h]	Maximum time in charge mode [min]	Maximum time in discharge mode [min]
Oct-22	73	0.3	0.3
Nov-22	68	0.2	0.4
Dec-22	83	0.3	0.4
Jan-23	71	0.2	0.3
Feb-23	59	0.3	0.1
Mar-23	36	4.6	5.6
Apr-23	26	4.3	0.9
May-23	70	0.4	0.3
Jun-23	72	1.3	0.7
Jul-23	60	0.8	0.4
Aug-23	145	1.3	1.8
Sep-23	100	1.0	0.5
Oct-23	125	0.9	1.4

Table 5.5 shows the total time in each of the analysed months that the EV battery would be in rest, charge, and discharge modes when considering the deviations outside the interval [49.9; 50.1] Hz. In this case, in a whole month the service would require the battery to charge/discharge an average of 10 minutes.

Table 5.5: Total time the EV battery is in rest, charge, and discharge modes when considering the deviations outside the interval [49.9; 50.1] Hz for the Continental synchronous area.

Month-Year	Total time in rest mode [days]	Total time in charge mode [min]	Total time in discharge mode [min]
Oct-22	31	6	2
Nov-22	30	3	4
Dec-22	31	3	7
Jan-23	31	2	4
Feb-23	28	4	2
Mar-23	31	30	35
Apr-23	30	38	21
May-23	31	7	6
Jun-23	30	11	7
Jul-23	31	8	4
Aug-23	31	8	11
Sep-23	30	5	7
Oct-23	31	7	5

Figure 5.2 presents the state-of-health variation considering the participation of an EV in the continental synchronous area, when the frequency deviations are outside the normal range in two different months.

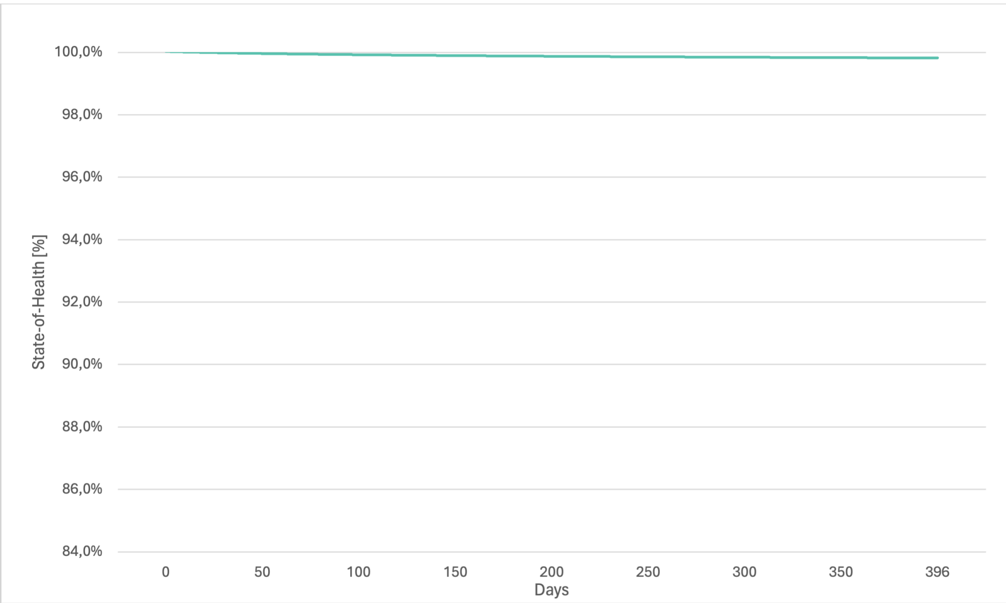

Figure 5.2: Battery State-of-Health considering the EV participation in Continental synchronous area frequency regulation outside the normal range from October 2022 to October 2023.

In this particular service, the state-of-health variation of the battery would be residual (around 0.04% a month), due to the frequency in this synchronous area being almost all the time within the range of

[49.9; 50.1] Hz, so the need for an EV to charge or discharge to compensate for any deviation would be small. And the main degradation mechanism in this service would be the calendar one.

It should also be noted that when these deviations occur, they do so in periods of a few seconds. This is not possible for a battery to respond because when a command to charge/discharge is sent it, generally, requires 2 or 3 seconds to react. Then the deviations would've been resolved, and the EV could not participate.

Table 5.6 presents the maximum time the EV would be in rest, charge, and discharge modes when considering the deviations outside the interval [49.9; 50.1] Hz for this area. It is evident that the maximum charge/discharge time required by the service would be approximately 1h10 (70 minutes) due to a single deviation event in the grid.

Table 5.6: Maximum time the EV is in rest, charge, and discharge modes when considering the deviations outside 50 Hz for the Continental synchronous area.

Month-Year	Maximum time in rest mode [min]	Maximum time in charge mode [min]	Maximum time in discharge mode [min]
Oct-22	0.2	48.0	49.7
Nov-22	0.2	59.3	43.3
Dec-22	0.2	50.0	39.5
Jan-23	0.2	40.0	66.1
Feb-23	0.2	37.7	26.4
Mar-23	0.2	59.8	48.3
Apr-23	0.1	46.4	60.7
May-23	0.0	29.0	41.9
Jun-23	0.0	32.3	55.8
Jul-23	0.0	33.6	31.4
Aug-23	0.2	70.1	55.0
Sep-23	0.2	40.1	64.2
Oct-23	64.2	40.1	23.3

Table 5.7 shows the total time in each of the analysed months that the EV battery would be in rest, charge, and discharge modes when considering the deviations outside the interval [49.9; 50.1] Hz. In this case, in a whole month the service would require the battery to charge/discharge at least half of the month, and rest a total of 13 hours, i.e. the battery would've almost all the time been needed to charge/discharge.

Table 5.7: Total time the EV battery is in rest, charge, and discharge modes when considering the deviations outside of 50 Hz for the Continental synchronous area.

Month-Year	Total time in rest mode [h]	Total time in charge mode [days]	Total time in discharge mode [days]
Oct-22	12	14	16
Nov-22	12	14	15
Dec-22	13	14	16
Jan-23	13	15	15
Feb-23	11	14	14
Mar-23	11	15	16
Apr-23	11	14	15
May-23	13	15	15
Jun-23	14	14	16
Jul-23	13	14	16
Aug-23	13	14	17
Sep-23	12	13	16
Oct-23	12	13	16

Based on Table 5.7 the demands of an EV battery in this service are very similar, because there isn't any month that stands out whether in much higher/lower rest mode time, or in much higher/lower total time in charge/discharge modes, therefore it was chosen to include the simulations results of the state-of-health between October 2022 to October 2023. This result is presented in Figure 5.3.

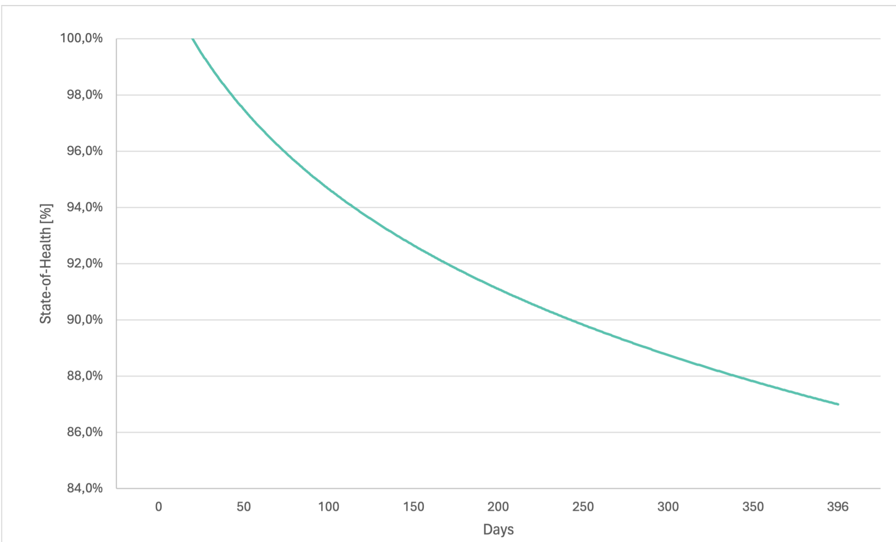

Figure 5.3: Battery State-of-Health considering the EV participation in Continental synchronous area continuous frequency regulation from October 2022 to October 2023.

In the case where we consider deviations outside of the nominal frequency, the state-of-health loss would be almost 14% a year, with a need to charge for a maximum of ±1 hour.

5.2.2 Nordic Synchronous Area

As done for the Continental synchronous area in the previous section, the simulations for the Nordic synchronous area were subdivided into those where the frequency deviations occur outside of the normal range, and those that are continuous, i.e. when the frequency is different than the nominal one.

Table 5.8 presents the maximum time the EV would be in rest, charge, and discharge modes when considering the deviations outside the interval [49.9; 50.1] Hz for this synchronous area. The maximum charge/discharge time required by the service would be almost an hour.

Table 5.8: Maximum time the EV is in rest, charge, and discharge modes when considering the deviations outside the interval [49.9; 50.1] Hz for the Nordic synchronous area.

Month-Year	Maximum time in rest mode [h]	Maximum time in charge mode [min]	Maximum time in discharge mode [min]
Oct-22	8.7	4.9	9.6
Nov-22	10.8	9.0	4.9
Dec-22	16.8	7.0	15.4
Jan-23	11.1	6.7	10.5
Feb-23	7.9	13.9	7.1
Mar-23	17.5	7.8	8.4
Apr-23	12.3	6.8	11.0
May-23	4.7	7.3	7.4
Jun-23	7.8	56.6	11.3
Jul-23	8.1	2.9	12.2
Aug-23	7.8	7.0	6.2
Sep-23	8.6	4.0	11.2
Oct-23	12.6	5.8	4.5

Table 5.9 shows the total time in each of the analysed months that the EV battery would be in rest, charge, and discharge modes when considering the deviations outside the interval [49.9; 50.1] Hz. In this case, in a whole month the service would require the battery to charge/discharge an average of 7 hours.

Table 5.9: Total time the EV battery is in rest, charge, and discharge modes when considering the deviations outside the interval [49.9; 50.1] Hz for the Nordic synchronous area.

Month-Year	Total time in rest mode [days]	Total time in charge mode [h]	Total time in discharge mode [h]
Oct-22	30	6	10
Nov-22	30	5	4
Dec-22	31	4	7
Jan-23	30	6	8
Feb-23	28	6	6
Mar-23	30	7	7
Apr-23	31	7	10
May-23	30	10	10
Jun-23	29	7	8
Jul-23	29	4	5
Aug-23	30	7	6
Sep-23	29	7	10
Oct-23	30	6	6

Figure 5.4 presents the state-of-health loss when considering the EV participation in the Nordic synchronous area, for frequency deviations outside of the nominal range, from October 2022 to October 2023.

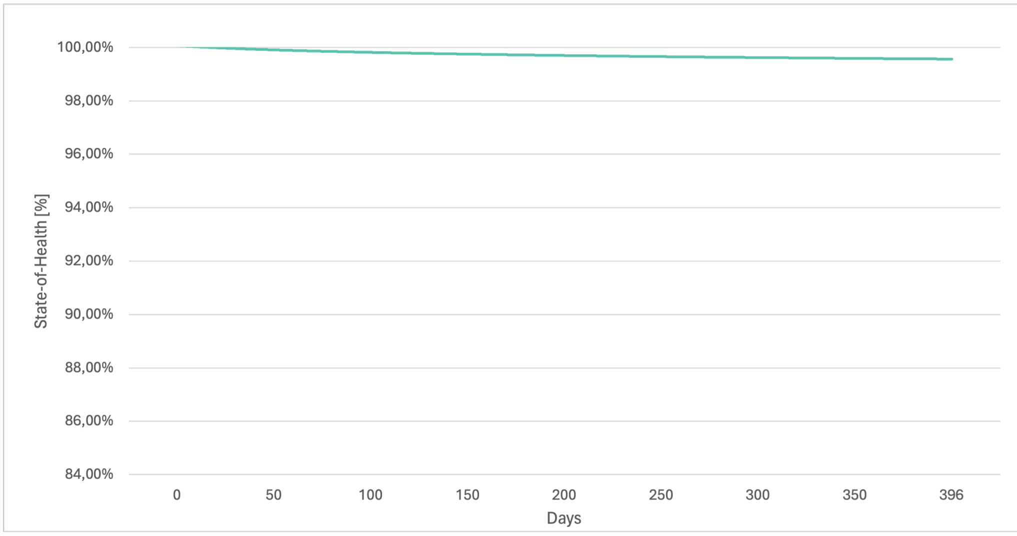

Figure 5.4: Battery State-of-Health considering the EV participation in Nordic synchronous area frequency regulation outside the normal range from October 2022 to October 2023.

With this service there would be a state-of-health loss of 0.5% a year.

Table 5.10 presents the maximum time the EV would be in rest, charge, and discharge modes when considering the deviations outside the interval [49.9; 50.1] Hz for this area. The maximum charge/discharge time required by the service would be around 1h30 (90 minutes) due to a single deviation event in the grid.

Table 5.10: Maximum time the EV is in rest, charge, and discharge modes when considering the deviations outside 50 Hz for the Nordic synchronous area.

Month-Year	Maximum time in rest mode [s]	Maximum time in charge mode [min]	Maximum time in discharge mode [min]
Oct-22	2	41.0	77.8
Nov-22	2	40.1	76.4
Dec-22	2	84.3	87.4
Jan-23	3	68.4	80.0
Feb-23	2	63.7	76.0
Mar-23	2	68.2	82.1
Apr-23	2	66.1	77.6
May-23	2	44.7	53.3
Jun-23	2	75.7	59.9
Jul-23	2	91.2	54.7
Aug-23	3	98.7	53.9
Sep-23	2	57.6	49.5
Oct-23	3	54.2	73.4

Table 5.11: Total time the EV battery is in rest, charge, and discharge modes when considering the deviations outside of 50 Hz for the Nordic synchronous area.

Month-Year	Total time in rest mode [s]	Total time in charge mode [days]	Total time in discharge mode [days]
Oct-22	0	16	15
Nov-22	0	15	15
Dec-22	0	16	15
Jan-23	0	16	15
Feb-23	0	14	14
Mar-23	0	15	15
Apr-23	0	15	15
May-23	0	16	15
Jun-23	0	15	15
Jul-23	0	15	15
Aug-23	0	15	15
Sep-23	0	15	15
Oct-23	0	16	15

Table 5.11 shows the total time in each of the analysed months that the EV battery would be in rest, charge, and discharge modes when considering the deviations outside the interval [49.9; 50.1] Hz. In this case, in a whole month the service would require the battery to charge/discharge at least half of the month, and no rest, i.e. the battery would've always been charging or discharging.

Figure 5.5 presents the state-of-health variation of a battery, considering the participation of the EV in the Nordic synchronous area in continuous frequency regulation, i.e. outside the nominal frequency.

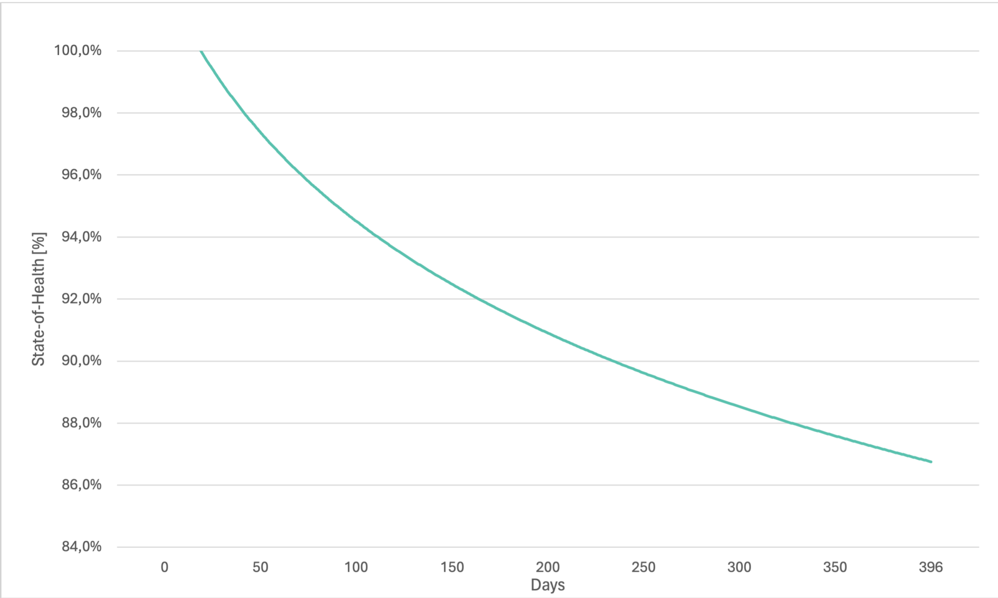

Figure 5.5: Battery State-of-Health considering the EV participation in Nordic synchronous area continuous frequency regulation from October 2022 to October 2023.

It can be observed from the last figure that this particular service would have a state-of-health loss for the battery of around 16% per year.

5.3 Flexibility Services

As previously mentioned, for the case of the flexibility services, which include local and electricity markets, dynamic contracts, and implicit and explicit demand response, it was considered for this work that in a worst scenario case, they would at maximum require the EV battery to do 2.5 cycles of charge/discharge in a day.

Figure 5.6 presents the state-of-health variation considering the EV participation in these flexibility services.

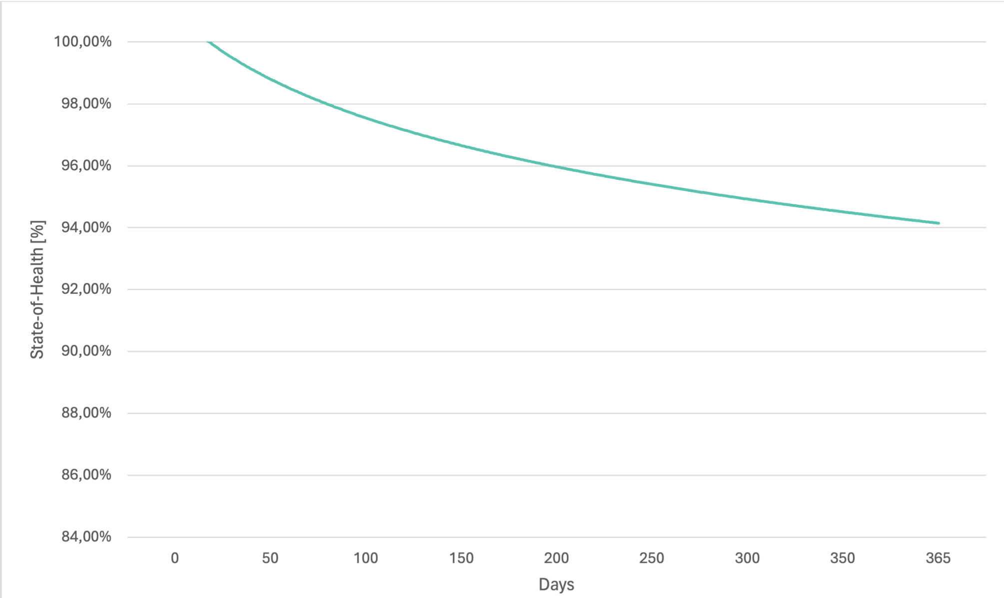

Figure 5.6: Battery State-of-Health considering the EV participation in flexibility services in a year.

From the obtained simulation it can be concluded that, in a worst-case scenario, the battery would lose 6% of state-of-health during a one-year period.

6 Conclusions

This deliverable presents a characterization of batteries degradation considering the participation in V2X services based on initial UCs, previously defined in the project. These services include wind curtailment, frequency regulation, local and flexibility markets, dynamic capacity contracts, and implicit and explicit demand response.

The proposed characterization used an extensive literature research, where a study of the services, the battery degradation and the models that exist was done, as a basis to then know that these services don't have the same demands for an EV battery, and therefore don't present the same impact on battery life.

In the performed simulations it was considered that the EV would always be available to perform these services.

6.1 Main Findings

One of the main findings of the present study is that there are two different aging mechanisms that need to be considered when studying the degradation of a battery, calendar, and cycle aging. This means that even when a battery isn't being used, there is a loss of capacity and power through time. But this loss can be lower than the one observed when considering the normal functioning of a battery, through charge and discharge cycles. So, when calculating the loss of state-of-health, these two mechanisms need to be considered to then have the full evaluation of a battery's degradation through time.

Another finding is that through the performed literature research, it was possible to use a semi-empirical battery degradation model that includes both the calendar and cycle aging. This model was then included in a simulation environment using a pre-existing python library, using each of the services conditions and requirements as input.

When concerning the V2X services' battery degradation, the main finding is that when studying each of the services and how the state-of-health of a battery would be affected with the use of an EV for these services. It was possible to see that each of the services can have a different impact.

Regarding wind curtailment, if an EV battery was always charged when there would be a need to curtail wind power, we could have up to 4% a year of state-of-health loss.

For the frequency regulation services, when considering the frequency deviations outside the normal range for the Continental and Nordic synchronous areas, there would be a state-of-health reduction per year of 0.3% and 0.5%, respectively. For the continuous frequency regulation outside of the nominal frequency, in the continental area there would be a loss of 16% a year, and in the Nordic area would also be around 16% a year.

When considering the flexibility services, that includes local markets, electricity markets, dynamic capacity contracts, implicit and explicit demand response, all of these would, to a battery, have the same expected demand. For this we considered a scenario where the battery would perform up to 2.5 cycles a day, which would mean a reduction in capacity of 8% a year.

So, it's possible to conclude that in the worst scenario of these services, if a battery was always being used to charge or discharge, we would have up to 16% a year of battery degradation. However, these types of applications will always make use of a fleet of EVs and not just one single vehicle, and therefore won't require that much demand on one battery, because they will be managed as a whole, and usually an EV wouldn't always be available for these services.

6.2 Main Challenges

One of the main challenges was to find a semi-empirical model that could be used in a simulation environment through a software tool or computing language library and encompassed the two degradation mechanisms of a battery in its mathematical form. There are a few models already in literature that try to do this, but they have some limitations, whether in the specificity of the cell's chemistry, data, or lack of standardization.

Another challenge was to find real data for each of the services, specially due to the flexibility services, where there aren't a lot of applications currently being used for a long time, so it's difficult to understand the real demands of them, which is why it was considered here a worst-case scenario for the simulations.

7 References

[1] European Comission, 'Deliverable 1.4 Business models centred in the V2X value chain', Mar. 2023. [Online]. Available: https://ev4eu.eu/wp-content/uploads/2023/09/D1.4-Business-models-centred-in-the-V2X-value-chain.pdf

[2] European Comission, 'Deliverable 1.5 V2X Use Cases Repository', Jun. 2023. [Online]. Available: https://ev4eu.eu/wp-content/uploads/2024/01/D1.5_V2X-Use-Cases-Repository.pdf

[3] N. Velosa *et al.*, 'Integration of Electric Vehicles in Electricity Markets and Flexibility Services: Business Use Cases Repository proposed in EV4EU project'. [object Object], Feb. 2024. doi: 10.5281/ZENODO.10675354.

[4] European Comission, 'Deliverable 2.1 Control Strategies for V2X Integration in Houses', Jun. 2023. [Online]. Available: https://ev4eu.eu/wp-content/uploads/2024/01/EV4EU-D2.1-Control-Strategies-for-V2X-Integration-in-Houses.pdf

[5] A. W. Thompson, 'Economic implications of lithium ion battery degradation for Vehicle-to-Grid (V2X) services', *J. Power Sources*, vol. 396, pp. 691–709, Aug. 2018, doi: 10.1016/j.jpowsour.2018.06.053.

[6] I. Nam, J.-H. Kim, Y. Yoo, and S. Jung, 'An EV-Based Wind Power Curtailment Scheme Utilizing the Power Sensitivity of the Distribution Network', *IEEE Access*, vol. 10, pp. 61124–61134, 2022, doi: 10.1109/ACCESS.2022.3181585.

[7] H. Bevrani, H. Golpîra, A. R. Messina, N. Hatziargyriou, F. Milano, and T. Ise, 'Power system frequency control: An updated review of current solutions and new challenges', *Electr. Power Syst. Res.*, vol. 194, p. 107114, May 2021, doi: 10.1016/j.epsr.2021.107114.

[8] J. Figgener *et al.*, 'The influence of frequency containment reserve flexibilization on the economics of electric vehicle fleet operation', *J. Energy Storage*, vol. 53, p. 105138, Sep. 2022, doi: 10.1016/j.est.2022.105138.

[9] L. Calearo and M. Marinelli, 'Profitability of Frequency Regulation by Electric Vehicles in Denmark and Japan Considering Battery Degradation Costs', *World Electr. Veh. J.*, vol. 11, no. 3, p. 48, Jul. 2020, doi: 10.3390/wevj11030048.

[10] Z. Hameed, C. Træholt, and S. Hashemi, 'Investigating the participation of battery energy storage systems in the Nordic ancillary services markets from a business perspective', *J. Energy Storage*, vol. 58, p. 106464, Feb. 2023, doi: 10.1016/j.est.2022.106464.

[11] M. Aziz and M. Huda, 'Utilization of electric vehicles for frequency regulation in Danish electrical grid', *Energy Procedia*, vol. 158, pp. 3020–3025, Feb. 2019, doi: 10.1016/j.egypro.2019.01.977.

[12] Energinet, 'Ancillary Services to be delivered in Denmark - Tender Conditions', Mar. 2023. [Online]. Available: https://en.energinet.dk/media/cmpnizek/ancillary-services-to-be-delivered-in-denmark-tender-conditions-20-04-2023.pdf

[13] P. A. V. Gade, T. Skjøtskift, H. W. Bindner, and J. Kazempour, 'Ecosystem for Demand-side Flexibility Revisited: The Danish Solution', *Electr. J.*, vol. 35, no. 9, p. 107206, Nov. 2022, doi: 10.1016/j.tej.2022.107206.

[14] ERSE, 'ERSE - Mercado'. [Online]. Available: https://www.erse.pt/eletricidade/funcionamento/mercado/

[15] N. Naval and J. M. Yusta, 'Virtual power plant models and electricity markets - A review', *Renew. Sustain. Energy Rev.*, vol. 149, p. 111393, Oct. 2021, doi: 10.1016/j.rser.2021.111393.

[16] Y. Su *et al.*, 'Research on Virtual Power Plant's Participation in Power Market under the Background of Energy Internet in China', *IOP Conf. Ser. Earth Environ. Sci.*, vol. 621, no. 1, p. 012015, Jan. 2021, doi: 10.1088/1755-1315/621/1/012015.

[17] B. Crowley, J. Kazempour, and L. Mitridati, 'Dynamic Pricing in an Energy Community Providing Capacity Limitation Services', 2023, doi: 10.48550/ARXIV.2309.05363.

[18] D. Newbery, 'Efficient Renewable Electricity Support: Designing an Incentive-compatible Support Scheme', *Energy J.*, vol. 44, no. 3, pp. 1–22, May 2023, doi: 10.5547/01956574.44.3.dnew.
[19] F. Gonzalez Venegas, M. Petit, and Y. Perez, 'Active integration of electric vehicles into distribution grids: Barriers and frameworks for flexibility services', *Renew. Sustain. Energy Rev.*, vol. 145, p. 111060, Jul. 2021, doi: 10.1016/j.rser.2021.111060.
[20] European Comission, 'Deliverable 1.6 Real-scale prototype of V2X management station'. [Online]. Available: https://ev4eu.eu/wp-content/uploads/2024/01/EV4EU-D1.6-Real-scale-prototype-of-V2X-management-station.pdf
[21] 'An Integrated Approach for Demand Response and Wind Curtailment Management in Distribution Systems', *Int. J. Renew. Energy Res.*, no. V13i2, 2023, doi: 10.20508/ijrer.v13i2.14197.g8734.
[22] NYISO, 'NYISO Demand Response Programs', Jun. 2020. [Online]. Available: https://www.nyiso.com/documents/20142/1398619/NYISO-Demand-Response-FAQs-for-Prospective-Resources.pdf/0377863d-84a6-de03-7486-f98e23f631e5
[23] Enefirst, 'Using Time-of-Use Tariffs to Engage Customers and Benefit the Power System'. [Online]. Available: https://enefirst.eu
[24] Poupa Energia, 'Poupa Energia - Tarifas e Ciclos horários'. [Online]. Available: https://poupaenergia.pt/tarifas-e-ciclos-horarios/
[25] Southern California Edison, 'Critical Peak Pricing'. [Online]. Available: https://www.sce.com/business/rates/cpp
[26] Luzigás, 'Tarifário de Referência'. [Online]. Available: https://www.luzigas.pt/tarifario-de-referencia/
[27] Department of Energy, 'Demand Response and Time-Variable Pricing Programs: Western States'. [Online]. Available: https://www.energy.gov/femp/demand-response-and-time-variable-pricing-programs-western-states
[28] X. Han *et al.*, 'A review on the key issues of the lithium ion battery degradation among the whole life cycle', *eTransportation*, vol. 1, p. 100005, Aug. 2019, doi: 10.1016/j.etran.2019.100005.
[29] A. Maheshwari, N. G. Paterakis, M. Santarelli, and M. Gibescu, 'Optimizing the operation of energy storage using a non-linear lithium-ion battery degradation model', *Appl. Energy*, vol. 261, p. 114360, Mar. 2020, doi: 10.1016/j.apenergy.2019.114360.
[30] L. Timilsina, P. R. Badr, P. H. Hoang, G. Ozkan, B. Papari, and C. S. Edrington, 'Battery Degradation in Electric and Hybrid Electric Vehicles: A Survey Study', *IEEE Access*, vol. 11, pp. 42431–42462, 2023, doi: 10.1109/ACCESS.2023.3271287.
[31] X. Liu, W. Ai, M. Naylor Marlow, Y. Patel, and B. Wu, 'The effect of cell-to-cell variations and thermal gradients on the performance and degradation of lithium-ion battery packs', *Appl. Energy*, vol. 248, pp. 489–499, Aug. 2019, doi: 10.1016/j.apenergy.2019.04.108.
[32] T. R. Ashwin, Y. M. Chung, and J. Wang, 'Capacity fade modelling of lithium-ion battery under cyclic loading conditions', *J. Power Sources*, vol. 328, pp. 586–598, Oct. 2016, doi: 10.1016/j.jpowsour.2016.08.054.
[33] A. Guha and A. Patra, 'Online Estimation of the Electrochemical Impedance Spectrum and Remaining Useful Life of Lithium-Ion Batteries', *IEEE Trans. Instrum. Meas.*, vol. 67, no. 8, pp. 1836–1849, Aug. 2018, doi: 10.1109/TIM.2018.2809138.
[34] S. Xiong, 'A study of the factors that affect lithium ion battery degradation', University of Missouri-Colombia, 2019.
[35] S. Barcellona and L. Piegari, 'Effect of current on cycle aging of lithium ion batteries', *J. Energy Storage*, vol. 29, p. 101310, Jun. 2020, doi: 10.1016/j.est.2020.101310.
[36] S. Saxena, Y. Xing, D. Kwon, and M. Pecht, 'Accelerated degradation model for C-rate loading of lithium-ion batteries', *Int. J. Electr. Power Energy Syst.*, vol. 107, pp. 438–445, May 2019, doi: 10.1016/j.ijepes.2018.12.016.

[37] J. Schmitt, M. Rehm, A. Karger, and A. Jossen, ‘Capacity and degradation mode estimation for lithium-ion batteries based on partial charging curves at different current rates’, *J. Energy Storage*, vol. 59, p. 106517, Mar. 2023, doi: 10.1016/j.est.2022.106517.
[38] J. Purewal, J. Wang, J. Graetz, S. Soukiazian, H. Tataria, and M. W. Verbrugge, ‘Degradation of lithium ion batteries employing graphite negatives and nickel–cobalt–manganese oxide + spinel manganese oxide positives: Part 2, chemical–mechanical degradation model’, *J. Power Sources*, vol. 272, pp. 1154–1161, Dec. 2014, doi: 10.1016/j.jpowsour.2014.07.028.
[39] K. Smith, M. Earleywine, E. Wood, J. Neubauer, and A. Pesaran, ‘Comparison of Plug-In Hybrid Electric Vehicle Battery Life Across Geographies and Drive Cycles’, presented at the SAE 2012 World Congress & Exhibition, Apr. 2012, pp. 2012-01–0666. doi: 10.4271/2012-01-0666.
[40] S. Grolleau *et al.*, ‘Calendar aging of commercial graphite/LiFePO4 cell – Predicting capacity fade under time dependent storage conditions’, *J. Power Sources*, vol. 255, pp. 450–458, Jun. 2014, doi: 10.1016/j.jpowsour.2013.11.098.
[41] G.-H. Kim, K. Smith, K.-J. Lee, S. Santhanagopalan, and A. Pesaran, ‘Multi-Domain Modeling of Lithium-Ion Batteries Encompassing Multi-Physics in Varied Length Scales’, *J. Electrochem. Soc.*, vol. 158, no. 8, p. A955, 2011, doi: 10.1149/1.3597614.
[42] S. A. Ashter, ‘Mechanics of Materials’, in *Thermoforming of Single and Multilayer Laminates*, Elsevier, 2014, pp. 123–145. doi: 10.1016/B978-1-4557-3172-5.00006-2.
[43] D. Del Olmo, M. Pavelka, and J. Kosek, ‘Open-Circuit Voltage Comes from Non-Equilibrium Thermodynamics’, *J. Non-Equilib. Thermodyn.*, vol. 46, no. 1, pp. 91–108, Jan. 2021, doi: 10.1515/jnet-2020-0070.
[44] D. U. Sauer and H. Wenzl, ‘BATTERIES | Lifetime Prediction’, in *Encyclopedia of Electrochemical Power Sources*, Elsevier, 2009, pp. 522–538. doi: 10.1016/B978-044452745-5.00852-2.
[45] P. Gyan *et al.*, ‘Experimental Assessment of Battery Cycle Life Within the SIMSTOCK Research Program’, *Oil Gas Sci. Technol. – Rev. D’IFP Energ. Nouv.*, vol. 68, no. 1, pp. 137–147, Jan. 2013, doi: 10.2516/ogst/2013106.
[46] J. Wang *et al.*, ‘Cycle-life model for graphite-LiFePO4 cells’, *J. Power Sources*, vol. 196, no. 8, pp. 3942–3948, Apr. 2011, doi: 10.1016/j.jpowsour.2010.11.134.
[47] J. Wang *et al.*, ‘Degradation of lithium ion batteries employing graphite negatives and nickel–cobalt–manganese oxide + spinel manganese oxide positives: Part 1, aging mechanisms and life estimation’, *J. Power Sources*, vol. 269, pp. 937–948, Dec. 2014, doi: 10.1016/j.jpowsour.2014.07.030.
[48] M. Marinelli, L. Calearo, and J. Engelhardt, ‘A Simplified Electric Vehicle Battery Degradation Model Validated with the Nissan LEAF e-plus 62-kWh’, in *Proceedings of 6th International Electric Vehicle Technology Conference*, 2023. [Online]. Available: https://findit.dtu.dk/en/catalog/641dad02819d663c28ee20aa